



1
2
3
4
5
6
7
8
9
10
11
12
13
14
15
16
17
18
19
20
21
22
23
24
25
26
27
28
29
30
31

Chikungunya intra-vector dynamics in *Aedes albopictus* from Lyon (France) upon exposure to a human viremia-like dose range reveals vector barrier's permissiveness and supports local epidemic potential

Barbara Viginier¹, Lucie Cappuccio¹, Céline Garnier¹, Edwige Martin², Carine Maisse¹, Claire Valiente Moro², Guillaume Minard², Albin Fontaine^{3,4,5}, Sébastien Lequime⁶, Maxime Ratinier¹, Frédérick Arnaud¹ & Vincent Raquin^{*1}

¹IVPC UMR754, INRAE, Université Claude Bernard Lyon 1, EPHE, PSL Research University, F-69007 Lyon, France.

² Université Claude Bernard Lyon 1, CNRS, INRAE, VetAgro Sup, UMR Ecologie Microbienne, F-69622 Villeurbanne, France.

³ Unité Parasitologie et Entomologie, Département Microbiologie et maladies infectieuses, Institut de Recherche Biomédicale des Armées (IRBA), Marseille, France.

⁴ Aix Marseille Univ, IRD, SSA, AP-HM, UMR Vecteurs-Infections Tropicales et Méditerranéennes (VITROME), Marseille, France.

⁵ IHU Méditerranée Infection, Marseille, France.

⁶ Cluster of Microbial Ecology, Groningen Institute for Evolutionary Life Sciences, University of Groningen, Groningen, The Netherlands.

*Corresponding author

Correspondence: vincent.raquin@ephe.psl.eu

NOTE: This preprint reports new research that has not been certified by peer review and should not be used to guide clinical practice.

32 **ABSTRACT**

33 Arbovirus emergence and epidemic potential, as approximated by the vectorial capacity formula,
34 depends on host and vector parameters, including the vector's intrinsic ability to replicate then
35 transmit the pathogen known as vector competence. Vector competence is a complex, time-
36 dependent, quantitative phenotype influenced by biotic and abiotic factors. A combination of
37 experimental and modelling approaches is required to assess arbovirus intra-vector dynamics
38 and estimate epidemic potential. In this study, we measured infection, dissemination, and
39 transmission dynamics of chikungunya virus (CHIKV) in a field-derived *Aedes albopictus*
40 population (Lyon, France) after oral exposure to a range of virus doses spanning human viraemia.
41 Statistical modelling indicates rapid and efficient CHIKV progression in the vector mainly due to
42 an absence of a dissemination barrier, with 100% of the infected mosquitoes ultimately
43 exhibiting a disseminated infection, regardless of the virus dose. Transmission rate data revealed
44 a time-dependent, but overall weak, transmission barrier, with individuals transmitting as soon
45 as 2 days post-exposure (dpe) and >50% infectious mosquitoes at 6 dpe for the highest dose.
46 Based on these experimental intra-vector dynamics data, epidemiological simulations conducted
47 with an agent-based model showed that even at low mosquito biting rates, CHIKV could trigger
48 outbreaks locally. Together, this reveals the epidemic potential of CHIKV upon transmission by
49 *Aedes albopictus* in mainland France.

50
51
52 **Keywords:** Arbovirus ; vector ; mosquito ; *Aedes albopictus* ; chikungunya virus ; epidemiology ; vector
53 competence ; modelisation

54

Introduction

56 Arthropod-borne viruses (arboviruses) are pathogens transmitted to vertebrate hosts by hematophagous
57 arthropods, mainly mosquitoes. Arbovirus spread is a multi-factorial, dynamic process that can be estimated
58 using the vectorial capacity (VCap) model, which aims to determine the average number of infectious vector
59 bites that arise per day from one infected host in a susceptible human population (Smith et al., 2012). The
60 vector-centric component of VCap integrates mosquito ecological (density per host, survival) and behavioural
61 (daily biting rate per human) factors along with the vector's proxies of virus transmission efficiency such as
62 vector competence (VComp) and its time-related expression, the extrinsic incubation period (EIP). VComp
63 represents the ability of mosquitoes to : i) allow midgut infection following an infectious blood meal, ii)
64 disseminate the virus beyond the midgut barrier, and iii) retransmit the virus through the saliva during the next
65 bite. In VCap models, VComp and EIP are often simplified under the EIP₅₀, the time required to reach 50% of
66 infectious mosquitoes. Effectively, each individual mosquito has a given EIP leading to a range of EIPs in the
67 population. EIP distribution can be assessed experimentally by measuring the time between the initial
68 mosquito infection and the mosquito infectiousness using an adequate experimental design (transmission
69 assay for a relevant number of individual mosquitoes and time points). Taking into account the time-
70 dependency of Vcomp improves VCap estimation and therefore allows to capture the full epidemic potential
71 of arboviruses (Lequime et al., 2020). VComp is impacted by biotic (e.g., mosquito and virus genotype, virus
72 dose, mosquito microbiota) and abiotic (e.g., temperature) factors (Viglietta et al., 2021), but how these
73 factors shape VComp dynamics has still to be determined.

74 Dengue virus (DENV), yellow fever virus (YFV), Zika virus (ZIKV), and chikungunya virus (CHIKV) pose a major
75 sanitary threat as they are responsible for hundreds of millions of human infections each year worldwide,
76 leading to severe morbidity and mortality (Labeaud et al., 2011; Bhatt et al., 2013). These arboviruses are
77 primarily transmitted to humans by *Aedes aegypti* mosquitoes, although the Asian tiger mosquito, *Aedes*
78 *albopictus*, is often incriminated as a vector. Indeed, *Ae. albopictus* is an important vector of arboviruses as
79 evidenced by vector competence laboratory assays and the detection of infected field specimens (Gratz, 2004;
80 Paupy et al., 2009). Notably, *Ae. albopictus* was identified as the main vector during CHIKV outbreaks in Gabon
81 (2007), Congo (2011) as well as in a major outbreak at La Réunion island (2006) (Schuffenecker et al., 2006;
82 Bonilauri et al., 2008; Pagès et al., 2009; Paupy et al., 2012; Mombouli et al., 2013). In Europe, this vector
83 species is incriminated for autochthonous circulation of CHIKV for instance in Italy (Venturi et al., 2017) and
84 mainland France (Delisle et al., 2015). Vector competence studies established that vector competence of *Ae.*
85 *albopictus* for CHIKV depends on genetic (e.g., mosquito and virus genotype) and environmental (e.g.,
86 temperature) factors (Tsetsarkin et al., 2007; Vazeille et al., 2007; Zouache et al., 2014; Sanchez-Vargas et al.,
87 2019). Host viremia, approximated by virus dose in the blood meal during artificial mosquito infectious feeding
88 experiments, is another major factor that drives mosquito vector competence (Nguyet et al., 2013; Aubry et
89 al., 2020). Vertebrate host viremia for CHIKV last 4 to 12 days with an increase in blood viral titer prior to
90 symptoms appearance, up to a peak around 8 log₁₀ infectious particles/mL followed by a decrease until virus
91 clearance for most of the cases (Schwartz & Albert, 2010). Beyond non-human primates, an estimate of CHIKV
92 human viremia dynamics is lacking due to limited longitudinal monitoring of infected patients, despite it could
93 help to decipher the duration and magnitude of human infectiousness for mosquitoes (Labadie et al., 2010).
94 In *Ae. albopictus*, two studies exposed mosquitoes to a range of CHIKV doses in the blood meal with varying
95 outcomes on vector competence as estimated by mosquito infection and dissemination rate (Pesko et al.,
96 2009; Hurk et al., 2010). Vector competence studies on *Ae. albopictus* from mainland France measured CHIKV
97 transmission rate although upon exposure to a single dose, always above 6.5 log₁₀ FFU/mL range which does
98 not cover the range of human viremia (Moutailler et al., 2009; Vega-Rua et al., 2013; Zouache et al., 2014;
99 Vega-Rúa et al., 2015). In addition, these studies focused on a limited number of time points after CHIKV
100 exposure that prevent to capture the dynamics of vector competence. A study monitoring intra-vector
101 dynamics of CHIKV and its epidemiological relevance is still lacking, notably upon variations of vector
102 competence major drivers such as virus dose.

103 Here, we studied intra-vector infection dynamics of a field-derived population of *Ae. albopictus* from Lyon
104 metropolis exposed by artificial membrane feeding to a range of human viraemia-like CHIKV (La Réunion 06.21
105 isolate, East Central South Africa (ECSA) clade) doses, based on our model of human CHIKV viremia in the
106 blood. Strains from ECSA clade carrying the same A226V mutation on envelope *E1* gene than 06.21 were
107 identified from autochthonous cases in mainland France, supporting the choice of the 06.21 strain for this study

108 (Franke et al., 2019). Individual mosquitoes were analyzed from day 2 to day 20 post-exposure (dpe) to
109 determine infection, dissemination, and transmission rates by infectious titration in addition to the
110 quantification of CHIKV RNA load in the saliva. This allowed us to estimate CHIKV intra-vector dynamics and
111 the strength of vector infection, dissemination, and transmission barriers as well as the distribution of EIP
112 according to the virus dose in the blood meal. These data were implemented in the agent-based model *nosoi*
113 (Lequime et al., 2020) to estimate, using realistic vectorial capacity parameters, the epidemic potential of
114 CHIKV in a French population of *Ae. albopictus*. Our results improve our understanding on vector-virus
115 interactions and provides key informations to better anticipate and prevent CHIKV emergence in mainland
116 France.

117 Methods

118 Modelling chikungunya viraemia in humans

119 Chikungunya virus (CHIKV) loads in human blood along with the time course of infection in patients were
120 recovered from two studies. The first study monitored blood CHIKV viraemia from a retrospective cohort of
121 102 febrile patients in Bandung, West Java, Indonesia, between 2005 and 2009 (Riswari et al., 2015). The
122 second study assessed CHIKV RNA viremic profile from 36 sera from day 1 to day 7 of illness during a CHIKV
123 epidemic in Thepa and Chana districts of Songkhla province, Thailand (Appassakij et al., 2013). For the
124 second study, the median value of the blood CHIKV RNA loads from a group of patients (n=2 to 21) per day of
125 illness was used. The viraemia data from RT-qPCR was expressed on the logarithmic scale to the base 10 before
126 model fitting. Wood's gamma-type function was used to model the viraemia dynamic. The function is given in
127 the following equation:

$$128 \quad y(t) = at^b e^{-ct} \text{ (Eq. 1)}$$

129
130
131 where $y(t)$ represents the level of viraemia in the blood at t days post-infection, with a , b , and c
132 representing constants linked to the viraemia dynamics (Islam et al., 2013). Viraemia data were originally
133 expressed in time pre- or post-symptom onset, while the model represents viraemia as a function of time post-
134 infection. A fixed arbitrary median intrinsic incubation period of 6 days was added to each viraemia time to
135 standardize the time scale between the data and the model. This fixed incubation period falls into the
136 estimated 2-10 days incubation range (Moloney et al., 2014) and was chosen to ensure that all observed
137 viraemia data occurred after infection. The model was fitted to the data using non-linear least-squares
138 regression implemented in the *nls* function in the R environment (RCORETeam, 2022). This method proposed a
139 possible intra-human CHIKV viraemia dynamic with 95% confidence intervals.

140 141 CHIKV stock production and titration

142 The CHIKV strain 06.21 from the Indian Ocean lineage was isolated from a newborn serum sample with
143 neonatal encephalopathy in La Réunion island in 2005 (Schuffenecker et al., 2006). This strain was amplified in
144 *Aedes albopictus* cell line C6/36 as previously described (Raquin et al., 2015). CHIKV was inoculated at a
145 multiplicity of infection of 0.01 on *Ae. albopictus* C6/36 cells cultivated in Leibovitz's L-15 media (Gibco) with
146 10 % (v:v) 1X Tryptose Phosphate Broth (Gibco), 10 % (v:v) foetal bovine serum and 0.1 % (v:v) 10,000 units/mL
147 penicillin/streptomycin (Gibco). Cells were incubated for 3 days at 28 °C before the cell supernatant was
148 clarified by centrifugation for 5 min at 500 g and stored at -80 °C as aliquots. CHIKV infectious titer was
149 measured on C6/36 using fluorescent focus assay (Raquin et al., 2015). Briefly, 3×10^5 cells/well were inoculated
150 in 96-well plates (TPP) with 40 µL/well of viral inoculum (after culture media removal) and incubated for 1 h at
151 28 °C. 150 µL/well of a mix 1:1 L-15 media and 3.2% medium viscosity carboxymethyl cellulose (Sigma) were
152 added as an overlay before incubation of the cells for 3 days at 28 °C. After incubation, cells were fixed in 150
153 µL/well of 4 % paraformaldehyde for 20 min at room temperature (RT) and then rinsed 3 times in 100 µL/well
154 of 1X Dulbecco's phosphate-buffered saline (DPBS) (Gibco) prior to immune labelling. Cells were permeabilized
155 for 30 min in 50 µL/well of 0.3 % (v:v) Triton X-100 (Sigma) in 1X DPBS + 1 % Bovine Serum Albumin (BSA,
156 Sigma) at RT then rinsed 3 times in 100 µL/well of 1X DPBS. A Semliki Forest virus anticapsid antibody cross-
157 reacting with CHIKV was used as a primary antibody, diluted 1:600 in 1X DPBS + 1 % BSA (Greiser-Wilke et al.,
158 1989). Cells were incubated in 40 µL/well of primary antibody for 1 h at 37°C, rinsed 3 times in 100 µL/well of
159 1X DPBS then incubated in 40 µL/well of anti-mouse Alexa488 secondary antibody (Life Technologies) at 1:500

160 in 1X DPBS + 1 % BSA for 30 min at 37 °C. Cells were rinsed 3 times in 100 µL/well 1X DPBS, then once in 100
161 µL/well tap water, stored at 4 °C overnight before the enumeration of fluorescent foci under Zeiss Colibri 7
162 fluorescence microscope at 10X objective. The CHIKV infectious titer was expressed as the log₁₀ fluorescent
163 focus unit (FFU) per mL. Plates were then stored at 4 °C protected from light to allow further reading. The
164 infectious titer of the neat CHIKV 06.21 stock was 8.63 log₁₀ FFU/mL.

165

166 **Mosquito colony maintenance**

167 The Lyon metropolis population of *Aedes albopictus* originates from a field sampling of larvae in 2018 that
168 were brought back to insectary for rearing (Microbial Ecology lab, Lyon, France). Sampling locations included
169 Villeurbanne (N : 45°46'18990" E : 4°53'24615") and Pierre-Bénite (N :45°42'11534" E : 4°49'28743") in Lyon
170 metropolis area, mainland France. Mass rearing of the population under standard laboratory conditions (28 °C,
171 80% relative humidity, 16:8 hours light:dark cycles) using mice feeding (*Mus musculus*) allowed to maintain
172 genetic diversity, in accordance with the Institutional Animal Care and Use Committee from Lyon1 University
173 and the French Ministry for Higher Education and Research (Apafis #31807-2021052715018315). Prior to
174 infectious blood feeding, eggs were hatched for 1 h in dechlorinated tap water, and larvae were reared at 26
175 °C (12:12h light:dark cycle) at a density of 200 larvae in 23 x 34 x 7 cm plastic trays (Gilac) in 1.5 L of
176 dechlorinated tap water supplemented with 0.1 g of a 3:1 (TetraMin tropical fish food:Biover yeast) powder
177 every two days. Adults were maintained in 32.5 x 32.5 x 32.5 cm mesh cages (Bugdorm) at 28 °C, 80 % relative
178 humidity, 12:12h light:dark cycle with permanent access to 10% sugar solution.

179

180 **Experimental mosquito exposure to CHIKV**

181 Female mosquitoes (4 to 8-day old) from F₁₀ generation were confined in 136 x 81 mm plastic feeding
182 boxes (Corning-Gosselin) with ~60 individual per box then transferred to the level 3 biosafety facility (SFR
183 Biosciences, AniRA-L3, Lyon Gerland) at 26 °C, 12:12 h light:dark cycle deprived from sugar solution 16 h before
184 the infectious blood meal. The blood meal was composed of a 2:1 (v:v) mixture of washed human erythrocytes
185 (from multiple anonymous donors collected by EFS AURA under the CODECOH agreement DC-2019-3507) and
186 viral suspension at several doses, and supplemented with 2 % (v:v) of 0.5 M ATP, pH 7 in water (Sigma). Feeders
187 (Hemotek) were covered with pig small intestine and filled with 3 mL of infectious blood mixture. Females
188 were allowed to feed for 1 h at 26 °C and blood aliquots were taken before (T0) and after (1h) the feeding and
189 stored at -80 °C for virus titration (Figure S1). Mosquitoes were anaesthetized on ice and fully engorged
190 females were transferred in 1-pint cardboard containers (10-25 females/container) and maintained with 10 %
191 sucrose. Cardboard containers were placed in 18 x 18 x 18 inches cages (BioQuip) and kept in climatic chambers
192 at 26 °C, 70 % humidity. Two independent vector competence experiments were conducted with 370 and 418
193 individuals mosquitoes per experiment, respectively. In a first experiment (n=370), mosquito body and head
194 infection were tested for the presence of infectious virus at 4 time points while in the second experiment
195 (n=418), mosquito head and saliva were analyzed at 10 time points.

196

197 **Mosquito dissection and CHIKV detection**

198 At the selected day post-exposure (dpe) to CHIKV, individual saliva were collected then the heads and
199 bodies were recovered. Prior to saliva collection, mosquitoes were anaesthetized on ice then legs and wings
200 were removed under a stereomicroscope. Individuals were placed on plastic plates maintained by double-
201 sided adhesive tape. The proboscis was inserted in a trimmed 10 µL filtered tip containing 10 µL of foetal
202 bovine serum (FBS) held above the mosquito by modelling clay (Heitmann et al., 2018). Two µL of 1 %
203 pilocarpine hydrochloride (Sigma) supplemented with 0.1 % Tween-20 (Sigma) in water were added on the
204 thorax of each mosquito to enhance salivation. Mosquitoes were allowed to salivate at 26 °C, 80 % relative
205 humidity for 1 h. The FBS that contains the saliva was expelled in an ice-cold tube filled with 150 µL of DMEM
206 media (Gibco) supplemented with antibiotics solution (Amphotericin B 2.5 µg/ml, Nystatin 1/100, Gentamicin
207 50 µg/ml, Penicillin 5 U/ml and Streptomycin 5 µg/ml (Gibco)). Following salivation, each mosquito's head and
208 body were separated using a pin holder with 0.15 mm minutien pins (FST). Heads and bodies were transferred
209 in individual grinding tubes (Qiagen) containing 500 µL of DMEM supplemented with antibiotics (see above)
210 and one 3-mm diameter tungsten bead (Qiagen). Samples were ground on a 96-well adapter set for 2 x 1 min,
211 30 Hz using a TissueLyser II (Qiagen), then stored at -80 °C. CHIKV detection was performed once on 40 µL of
212 undiluted (raw) saliva, head and body samples using fluorescent focus assay on C6/36 cells (see above). Each
213 mosquito sample was declared positive or negative for CHIKV in the presence or absence of a fluorescent

214 signal, respectively. Each 96-well plate contained positive (virus stock) and negative (raw grinding media)
215 controls. Two independent persons examined each plate. Of note, saliva samples were deposited immediately
216 (no freezing step) on C6/36 cells to maximize CHIKV detection. 30 μ L of saliva sample were immediately mixed
217 with 70 μ L of TRIzol (Life Technologies) and stored at -80°C before RNA isolation. The rest of the samples were
218 stored at -80°C as a backup.

219

220 RNA isolation from saliva

221 Total RNA was isolated from 30 μ L of saliva mixed with 70 μ L TRIzol and then stored at -80°C , as described
222 (Raquin et al., 2017). After thawing samples on ice, 20 μ L chloroform (Sigma) were added. The tubes were
223 mixed vigorously, incubated at 4°C for 5 min and centrifuged at 17,000 G for 15 min, 4°C . The upper phase
224 was transferred in a new tube containing 60 μ L isopropanol supplemented with 1 μ L GlycoBlue (Life
225 Technologies). Samples were mixed vigorously and stored at -80°C overnight to allow RNA precipitation. After
226 15 min at 17,000 G, 4°C , the supernatant was discarded, and the blue pellet was rinsed with 500 μ L ice-cold
227 70 % ethanol in water. The samples were centrifuged at 17,000 G for 15 min, 4°C , the supernatant was
228 discarded, and the RNA pellet was allowed to dry for 10 min at room temperature. Ten μ L RNase-free water
229 (Gibco) were added, and samples were incubated at 37°C for 10 min to solubilize RNA prior to transfer in
230 RNase-free 96-well plates and storage at -80°C .

231

232 CHIKV RNA load quantification in saliva

233 Total RNA (2 μ L) isolated from individual mosquito saliva were used as template in a one-step TaqMan RT-
234 qPCR assay. The QuantiTect Virus kit (Qiagen) was used to prepare the reaction mix in a final volume of 30 μ L.
235 The reaction solution consisted of 6 μ L 5X master mix, 1.5 μ L primers (forward 5'-CCCGGTAAGAGCGGTGAA-3'
236 and reverse 5'-CTTCCGGTATGTCGATGGAGAT-3') and TaqMan probe (5'-6FAM-TGCGCCGTAGGGAACATGCC-
237 BHQ1-3') (Hurk et al., 2010) mixed at 0.4 μ M and 0.2 μ M final concentration respectively, 0.3 μ L 100X RT mix,
238 20.2 μ L RNase-free water (Gibco) and 2 μ L template saliva RNA. RT-qPCR reaction was conducted on a Step
239 One Plus machine (Applied) for 20 min at 50°C (RT step), 5 min at 95°C (initial denaturation) and 40 cycles with
240 15 s at 95°C and 45 s at 60°C . Serial dilutions of CHIKV 06.21 synthetic RNA from 8 to 1 \log_{10} copies/ μ L were
241 used as an external standard to estimate CHIKV RNA copies in saliva samples. Each plate contained duplicates
242 of standard synthetic RNA samples as well as negative controls and random saliva samples without reverse
243 transcriptase (RT-) also in duplicate. Aliquots from the same standard RNA (thawed only once) were used for
244 all the plates, and samples from a single time-point were measured on the same plate to allow sample
245 comparison.

246

247 Statistical analyses

248 Mosquito infection (number of CHIKV-positive mosquito bodies / number engorged mosquitoes),
249 dissemination (number of CHIKV-positive heads / number of CHIKV-positive bodies) and transmission rate
250 (number of positive CHIKV-saliva / number of CHIKV-positive heads) were analysed by logistical regression and
251 considered as binary response variables. The time (dpe) and virus dose (\log_{10} FFU/mL) were considered
252 continuous explanatory variables in a full factorial generalized linear model with a binomial error and a logit
253 link function. Logistic regression assumes a saturation level of 100% and could not be used to model the
254 relationship between the probability of transmission (response variable) and the time post-infection, the dose
255 and their interaction (predictors). Therefore, we first estimated the saturation level (K) for each dose and
256 subtracted the value $N = \text{number of mosquitoes with CHIKV dissemination} \times (100\% - K)$ to the number of
257 mosquitoes without virus in their saliva at each time post virus exposure to artificially remove mosquitoes that
258 would never ultimately transmit the virus from the dataset. Logistic regression was then used on these
259 transformed data to predict transmission rates across time post virus exposure and the virus dose (Figure S2).
260 The statistical significance of the predictors' effects was assessed by comparing nested models using deviance
261 analysis based on a chi-squared distribution. All the statistical analyses were performed in R Studio (Posit), and
262 figures were created with the package *ggplot2* within the *Tidyverse* environment (Wickham et al., 2019). The
263 R script used for this study is available, and supplementary table 1 summarizes the proportion of infected,
264 disseminated and infectious mosquitoes for all the experiments conducted.

265

266 Epidemiological modelling using *noso*

267 A series of stochastic agent-based model simulations were performed using the R package *nosoi* and a
268 specific branch available on *nosoi*'s GitHub page (<https://github.com/slequime/nosoi/tree/fontaine>) as
269 previously done (Lequime et al., 2020). Briefly, 100 independent simulations were run in replicates for each
270 condition. Each simulation started with one infected human and was run for 365 days or until the allowed
271 number of infected individuals (100,000 humans or 1,000,000 mosquitoes, respectively) was reached. We
272 considered transmission only between an infected mosquito and an uninfected human or between an infected
273 human and an uninfected mosquito. Vertical and sexual transmission, and the impact of potential
274 superinfection were ignored during the simulations. We assumed no particular structure within host and
275 vector populations.

276 It was also considered that humans do not die from infection and leave the simulation after they clear the
277 infection (here 12 days). Each human agent experienced a Poisson-like distribution of bites per day with a
278 mean value manually set at 1, 2, 3, 4, 5, 6, 7, 8, 9, 10 or 60 based on field measurement of *Aedes albopictus*
279 blood-feeding behaviour (Delatte et al., 2010). Human-to-mosquito transmission followed a time-post-
280 infection-dependent probability function, identical for all human agents, computed from the human viraemic
281 profile (Eq. 1, see above) and dose-response experiments (Eq. 2) :

$$282 \quad 283 \quad p_{trans\ H \rightarrow M}(t) = \frac{1}{1 + \exp(-(-11.1678 + 1.9929 * (a * t^b * \exp(-c * t))))} \quad (\text{Eq. 2})$$

284 where based on our model, $a = 0.01479$, $b = 7.21809$ and $c = 1.11915$.

285
286 The daily survival probability of infected mosquito agents was set empirically at 0.85 (Favier et al., 2005;
287 Fontaine et al., 2018). Human biting (only one per mosquito agent) was set at fixed dates depending on a
288 gonotrophic cycle duration drawn for each mosquito in a truncated Poisson distribution with a mean of 4 days
289 (no draws below 3). The mosquito-to-human transmission was determined for each mosquito agent based on
290 its individual EIP value acting as a threshold for transmission (if time post-infection is greater or equal to the
291 EIP value, the mosquito can transmit). However, a certain proportion (based on saturation parameter K, see
292 above) of mosquitoes never transmitted. The individual EIP value was dependent on the virus dose that
293 initiated the infection based on this equation (Lequime et al., 2020):

$$294 \quad 295 \quad DD50 = \frac{(\log(\frac{-P}{P-1.001}) - \beta_0 - \beta_1 \times X1)}{\beta_2 + \beta_3 \times X1} \quad (\text{Eq. 3})$$

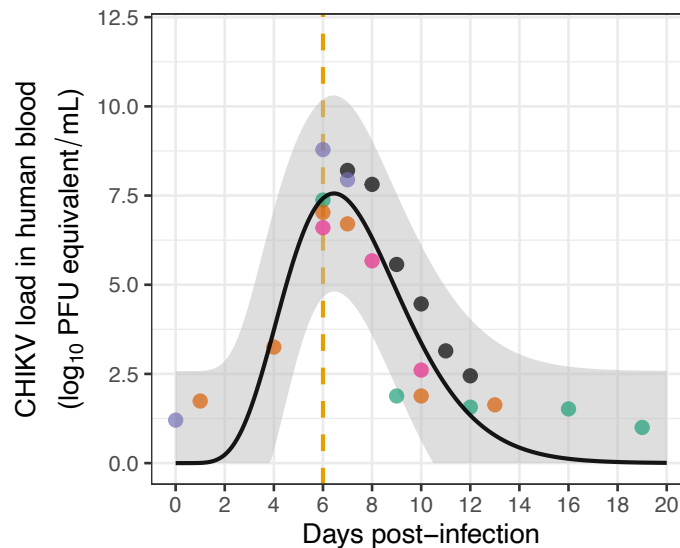
296 where $P = 0.5$ (i.e., the median transmission probability), β_0 is the Y-intercept value (-2.328973), β_1
297 (0.278953), β_2 (0.136746) and β_3 (0.003276) are model coefficients associated to the virus dose, time post virus
298 exposure and their interaction, respectively. $X1$ represents the virus dose value.

301 Results

302 Estimating CHIKV viraemia in humans by modelisation of clinical data

303 Intra-human dynamic of CHIKV viraemia over time post-infection was approximated using time course of
304 human CHIKV viraemia in individual patients from two studies (Appassakij et al., 2013; Riswari et al., 2015).
305 CHIKV loads were assessed at 3 to 6 different time points, prior or post symptoms onset from the blood of 5
306 patients. The range of CHIKV viraemia duration among the 5 patients was 4-12 days, with a minimal and a
307 maximum CHIKV load of 1 and 8.78 \log_{10} PFU equivalent/mL, respectively. Of note, two patients displayed 1.04
308 and 3.25 \log_{10} PFU equivalent/mL before symptoms onset, respectively. Modelling CHIKV viraemic profile using
309 a Wood's gamma-type function indicates that mean viral load rapidly increases to peak after 6.45 days (i.e.
310 within 24 h after symptoms onset) at 7.55 \log_{10} PFU equivalent/mL (7.01-8.78 \log_{10} equivalent PFU/mL
311 depending on the patient) (Figure 1).

312

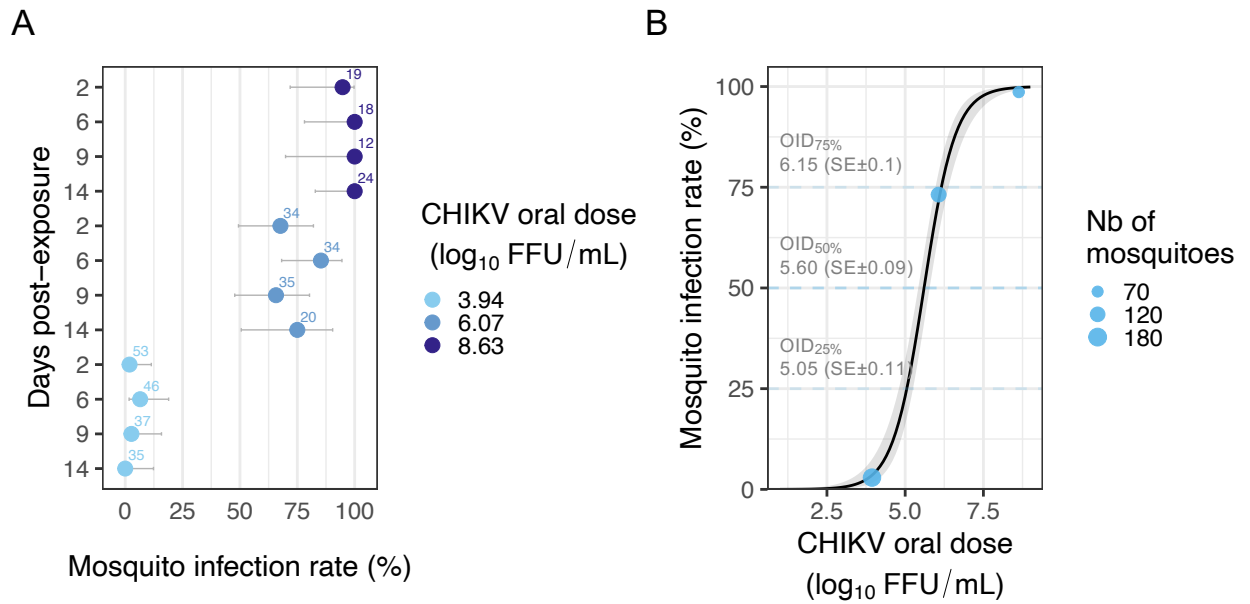


313
314
315
316
317
318
319
320
321
322
323

Figure 1 - Estimated time course of CHIKV load in human blood as a function of days post-infection. A Wood's gamma-type function was used to model CHIKV viraemia dynamics based on the time course of human viraemia data in 5 patients. The black line represents model prediction using mean fit parameter values. Each dot represents a single experimental measurement with colours corresponding to different patients. The vertical gold line indicates the day of symptoms onset. The grey ribbon represents upper and lower predicted values. Refers to raw data table "ChikV_Viremia_dynamic.txt" (see data availability section).

324 **The dose, but not the time, modulates mosquito infection rate**

325 Female *Ae. albopictus* were separately exposed to a human erythrocytes suspension containing three CHIKV
326 doses (3.94, 6.07 and 8.63 log₁₀ FFU/mL) that span the estimated range of human viraemia as estimated above
327 (Figure 1). The mortality rate was very low regardless of time or oral dose, remaining below 5%. Mosquito
328 infection rate (IR) remained below 7 % (n=35 to 53 individuals tested) at 3.94 log₁₀ FFU/mL, ranged from 65 to
329 85 % at 6.07 log₁₀ FFU/mL (n=20 to 35) and raised above 94 % at 8.63 log₁₀ FFU/mL (n=12 to 24) (Figure 2A). A
330 detail table of these data is presented in supplementary table S1. IR significantly increases with the dose but
331 it does not depend on the time post-exposure (Wald χ^2 , $P_{\text{dose}} = 1.1 \times 10^{-6}$, $P_{\text{time}} = 0.9$ and $P_{\text{dose*time}} = 0.17$). As IR
332 depends on the virus dose but not on the time post-exposure, we fitted a logistic model to the data considering
333 CHIKV titer in the blood meal as a unique explanatory variable (Figure 2B). Dose-dependent IR describes a
334 sigmoid with a median oral infection dose (OID_{50%}) of 5.6 log₁₀ FFU/mL and an OID_{25%} and OID_{75%} of 5.05 log₁₀
335 FFU/mL and 6.15 log₁₀ FFU/mL, respectively. The oral infection saturation level was reached at about 7.5 log₁₀
336 FFU/mL.
337



338
339

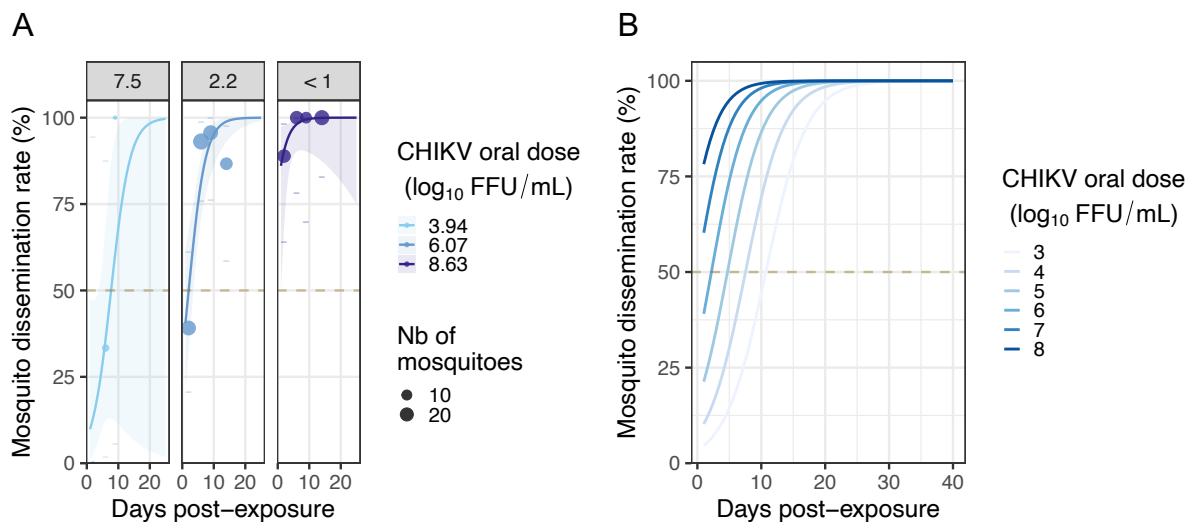
340 Figure 2 - Dose-dependent infection rate of *Ae. albopictus* mosquitoes exposed to
 341 CHIKV 06.21. (A) The mosquito infection rate corresponds to the proportion (in %) of
 342 mosquito bodies positive for CHIKV infection out of the total of engorged mosquitoes,
 343 measured at 2, 6, 9 and 14 days post-exposure for three CHIKV doses (3.94, 6.07 and 8.63
 344 log₁₀ FFU/mL) in the blood meal. The number of individuals analysed at each time point is
 345 indicated above the bars that represents the 95% confidence interval. (B) Mosquito
 346 infection rate as a function of CHIKV dose in the blood meal. Blue dots correspond to the
 347 observed infection rate upon the three CHIKV doses tested. Dot size is proportional to the
 348 number of mosquitoes tested. The black line was obtained by fitting a logistic model to the
 349 data. The grey ribbon indicates the 95 % confidence interval. The oral infectious dose (OID)
 350 to infect 25 %, 50 % and 75 % of the mosquitoes exposed to CHIKV is indicated with the
 351 associated standard error (in log₁₀ FFU/mL). Refers to raw data table
 352 "Data_titer_EIPdyna_body_head_final.txt" (see data availability section).
 353

353

354 Dose- and time-dependent mosquito dissemination dynamics

355 The proportion of CHIKV-positive heads among positive bodies (*i.e.*, mosquito dissemination rate, DIR) was
 356 analysed using virus dose, time post-exposure and their interaction as explanatory variables. At 2 days post-
 357 exposure, <50 % of the mosquitoes presented a disseminated infection for the doses 3.94 (n=1 individual
 358 tested) and 6.07 (n=18) log₁₀ FFU/mL, whereas DIR was already above 80 % after 2 days in mosquitoes exposed
 359 to 8.63 log₁₀ FFU/mL of CHIKV (n=23) (Figure 3A). Notably, DIR increases >80 % for all the three doses after 6
 360 dpe (n=1 to 29 individual tested per time point and dose) (Figure 3A and Table S1). Although they are not in
 361 interaction, both time and dose impact DIR (Wald χ^2 , $P_{\text{dose}} = 8.29 \times 10^{-6}$, $P_{\text{time}} = 1.75 \times 10^{-6}$ and $P_{\text{dose*time}} = 0.83$).
 362 The plateau was 100 % at doses 3.94 and 8.63 log₁₀ FFU/mL and 95.6% at the dose 6.07 log₁₀ FFU/mL (n=22/23).
 363 The time to reach 50 % dissemination in *Ae. albopictus* exposed to CHIKV was 7.5 days, 2.2 days and <1 day for
 364 3.94, 6.07 and 8.63 log₁₀ FFU/mL CHIKV doses in the blood meal, respectively. DIR was inferred from
 365 experimental data for a larger set of CHIKV dose ranging from 3 to 8 log₁₀ FFU/mL (Figure 3B). All the CHIKV
 366 doses tested led to 100% dissemination within the 40 days range used for predictions, although a longer time
 367 is required to reach this plateau at the lowest dose.
 368

368



369
370

371

372

373

374

375

376

377

378

379

380

381

382

383

384

385

Figure 3 - Dose-dependent dissemination rate of *Ae. albopictus* mosquitoes exposed to CHIKV 06.21. (A) The mosquito dissemination rate corresponds to the number of CHIKV-positive heads out of the infected (CHIKV-positive bodies) individuals, measured at 2, 6, 9 and 14 days post-exposure for three virus doses (3.94, 6.07 and 8.63 log₁₀ FFU/mL) in the blood meal. Dot size is proportional to the number of mosquitoes tested. No disseminated females were detected at day 14 post-exposure at the 3.94 log₁₀ FFU/mL dose. Logistic regression was used to model the time-dependent effect of the virus dose on mosquito dissemination rate. Lines correspond to fit values with their 95% confidence intervals displayed as ribbons. The time needed to reach 50 % dissemination is 7.5, 2.2 and <1 day for the 3.94, 6.07 and 8.63 log₁₀ FFU/mL CHIKV doses, respectively, as indicated within each facet label. (B) Predicted dissemination dynamics according to virus dose and time post-exposure for a range of CHIKV blood meal titers (3 to 8 log₁₀ FFU/mL). Refers to raw data table "Data_titer_EIPdyna_final.txt" (see data availability section).

386

Time post-exposure modulates transmission rate and viral load in the saliva

387

388

389

390

391

392

393

394

395

396

397

398

399

400

401

402

403

404

405

406

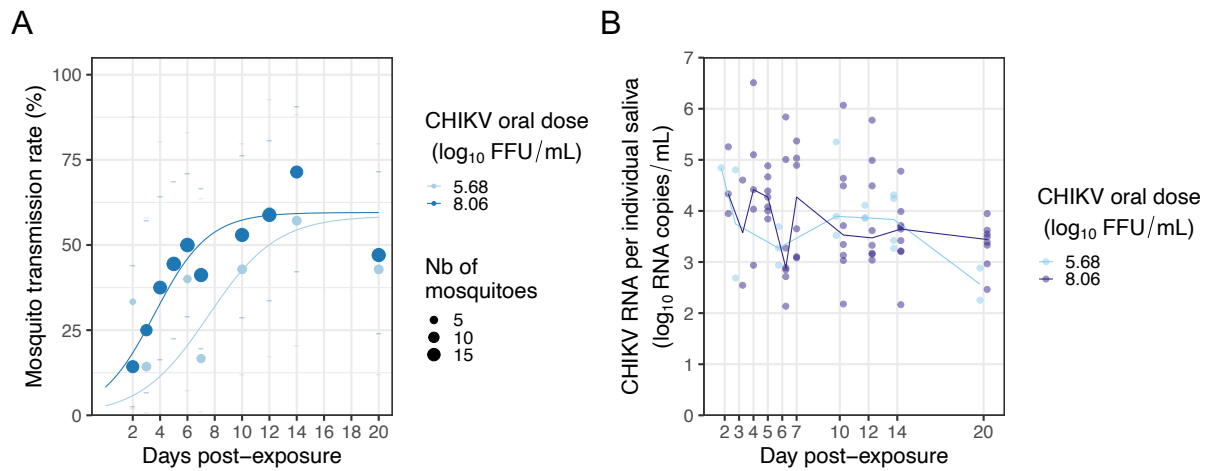
407

408

The presence of infectious CHIKV particles in individual mosquito saliva collected by forced salivation technique was monitored at a fine time scale. This allowed us to measure the transmission rate (TR) and quantify individual viral load in saliva over time, and to estimate the extrinsic incubation period (EIP). Two virus doses (5.68 and 8.06 log₁₀ FFU/mL) were used to obtain a workable proportion of infectious mosquitoes at a high number of time points that covers mosquito expected lifespan while remaining in the range of human viraemia. From day 2 post-exposure, TR increases following a sigmoid shape, reaching a plateau of around 60% for both doses (Figure 4A). TR was analysed using virus dose, time post-exposure and their interaction as explanatory variables, and only time was significant (Wald χ^2 , $P_{\text{time}} = 0.0037$, $P_{\text{dose}} = 0.18$, and $P_{\text{dose*time}} = 0.8$). Infectious saliva samples were detected as soon as day 2 post-exposure to CHIKV, with a 33 % TR at dose 5.68 log₁₀ FFU/mL (n=1/3 individuals tested) and 14 % at dose 8.06 log₁₀ FFU/mL (n=2/14). The time needed to reach 50 % infectious mosquitoes (*i.e.* Extrinsic Incubation Period 50%, EIP_{50%}) was 7.5 and 3.5 days for doses 5.68 and 8.06 log₁₀ FFU/mL, respectively. A TR saturation at 100 % is a prerequisite to applying logistic regression analysis to the data. Therefore, the proportion of mosquitoes that would not ultimately transmit the virus was artificially removed from the dataset based on the predicted saturation level at each dose (*i.e.*, 40 % of mosquitoes without the virus in their saliva were removed at each time post-infection). Logistic regression was used on these transformed data to predict TR across a range of doses over time (Figure S2).

To decipher if CHIKV load in the saliva could be associated with the virus dose mosquitoes were challenged with, total RNA was isolated at each time point from the saliva of individual mosquitoes exposed to 5.68 or 8.06 log₁₀ FFU/mL. Viral load was measured by TaqMan RT-qPCR assay and analysed according to virus dose and time post-exposure. A high individual variation is noticed (up to 10,000 fold difference between individuals), although CHIKV load in the saliva seems to decrease over time (Figure 4B). Only the time post-exposure significantly affected viral load when considering saliva samples that were CHIKV-positive both in qRT-PCR and in infectious titration (Anova, $P_{\text{time}} = 0.006$, $P_{\text{dose}} = 0.66$ and $P_{\text{dose*time}} = 0.94$). Of note, both time

409 and virus dose affected viral load in the saliva when considering RNA-positive samples regardless of the
410 presence of infectious virus (Figure S3).
411



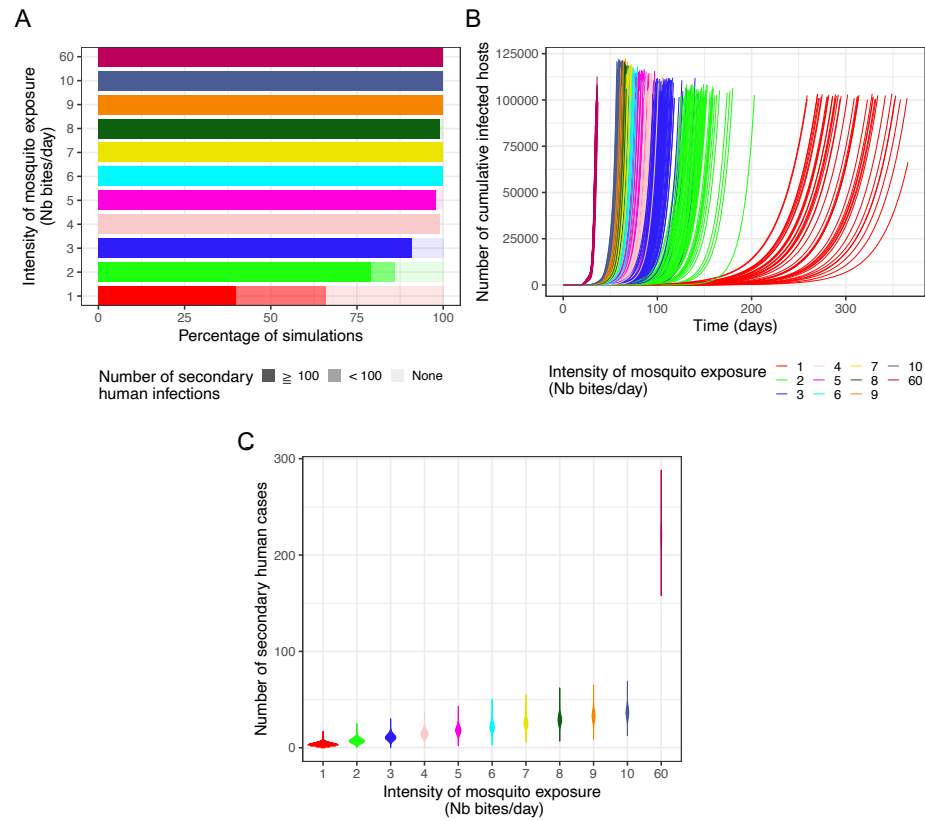
412
413

414 Figure 4 - Transmission dynamics of CHIKV 06.21 by *Ae. albopictus*. (A) Mosquito
415 transmission rate corresponds to the number of CHIKV-positive saliva out of the number
416 of CHIKV-positive heads collected at 2, 3, 4, 5, 6, 7, 10, 12, 14, and 20 days post-exposure
417 for two virus doses (5.68 and 8.06 log₁₀ FFU/mL) in the blood meal. Dot size is proportional
418 to the number of saliva tested. (B) CHIKV RNA load of each saliva scored positive for
419 infectious CHIKV was measured by TaqMan RT-qPCR assay using a synthetic RNA as
420 standard, then expressed in log₁₀ CHIKV RNA copies/saliva. Each dot represents a saliva
421 sample from a mosquito exposed to the indicated dose. Refers to raw data tables
422 “Data_titer_EIPdyna_final.txt” and “Data_CHIKV_RNA_load_saliva.txt” (see data
423 availability section).
424

425

425 Simulation of CHIKV epidemic upon dose-dependent intra-vector dynamics

426 A stochastic agent-based model was used to assess the epidemiological impact of within-host CHIKV
427 dynamics using the R package *nosoi*, as done previously for ZIKV (Lequime et al., 2020). Starting with one
428 infected human in a population of susceptible humans and mosquitoes, the model simulates CHIKV
429 transmissions according to human viraemia, its derived probability of mosquito infection, and virus
430 transmission timeliness (EIP). The model was run 100 independent times for a maximum of 365 days for a
431 range of eleven mean individual mosquito biting rates (1, 2, 3, 4, 5, 6, 7, 8, 9, 10 and 60 independent
432 mosquitoes biting per person per day). Simulations led to large outbreaks (>100 secondary infections) even
433 under a low mosquito biting rate (Figure 5A). The maximum threshold of mosquito infection was reached
434 regardless of biting intensity, although the time needed to reach this threshold and the inter-simulation
435 variation were higher at the lowest biting intensity (*i.e.* 1 bite per day) compare to other conditions (Figure
436 5B). Accordingly, secondary cases values distributions across simulations were narrow for all conditions except
437 at 1 bite per day reflecting the explosive nature of the outbreak. The mean secondary case values increases as
438 a function of the mosquito biting intensity with a mean (\pm SD) of 3.68 (\pm 1.92), 7.37 (\pm 2.71), 11.06 (\pm 3.32),
439 14.75 (\pm 3.84), 18.43 (\pm 4.29), 22.12 (\pm 4.7), 25.81 (\pm 5.07), 29.5 (\pm 5.43), 33.18 (\pm 5.75), 36.87 (\pm 6.07) and
440 221.15 (\pm 6.09) for 1, 2, 3, 4, 5, 6, 7, 8, 9, 10 and 60 mosquito bites per person per day, respectively (Figure 5C).
441



442
443
444
445
446
447
448
449
450
451
452
453
454

Figure 5 - Influence of dose-dependent intra-mosquito CHIKV dynamics on outbreak simulations with various levels of mosquito bites. Stochastic agent-based epidemiological simulations considering within-vector infection dynamics on transmission probability during mosquito-human infectious contacts were performed in 100 independent replicates. A total of 11 mosquito bite intensity levels were tested: 1, 2, 3, 4, 5, 6, 7, 8, 9, 10 and 60 bites per human per day. (A) Stacked proportions of outbreak simulations resulting in no secondary infected human host, < 100 and ≥ 100 infected human hosts. (B) Cumulative number of infected humans over time. Each curve represents a simulation run. (C) Violin plots showing the number of secondary cases densities for each intensity of mosquito exposure. Refers to raw data tables "Compiled_results_run5.csv", "cumulative_run5.csv" and "R0dist_run5.csv" (see data availability section).

456 Vector competence (VComp) of *Aedes albopictus* for chikungunya virus (CHIKV) has been widely
457 studied, notably since the La Réunion outbreak in 2006. Studies outlined a strong impact of mosquito and
458 CHIKV genotype as well as temperature on *Ae. albopictus* potential for CHIKV transmission, including large
459 VComp variations among worldwide *Ae. albopictus* populations exposed to the highly transmissible La
460 Réunion 2006 CHIKV 06.21 isolate (Zouache et al., 2014; Mariconti et al., 2019; Gloria-Soria et al., 2020;
461 Vega-Rúa et al., 2020). However, knowledge gaps remain regarding intra-vector virus dynamics and its
462 impact on CHIKV epidemic potential notably regarding the virus dose. Our work contributes to fill these
463 gaps, providing important data on the interplay between CHIKV and *Ae. albopictus* as well as on the
464 viremia-dependent human infectiousness for mosquitoes.

465

466 Dose and time-dependent barriers to CHIKV intra-vector dynamics

467 *Ae. albopictus* midgut infection is strongly influenced by CHIKV dose in the blood meal. Previous studies
468 documented an oral infectious dose for 50 % of the mosquitoes (OID_{50%}) ranging from 1.7 to 3.52 log₁₀
469 infectious particles per mL of blood for CHIKV 06.21 and thus lower than the 5.60 log₁₀ FFU/mL OID_{50%}
470 estimated in our *Ae. albopictus* population (Tsetsarkin et al., 2007; Pesko et al., 2009; Hurk et al., 2010).
471 ZIKV OID_{50%} was 5.62 log₁₀ FFU/mL in *Ae. albopictus* while in *Ae. aegypti*, ZIKV and DENV OID_{50%} ranged
472 from 4.73 to 8.10 log₁₀ FFU/mL and from 3.95 to 5.5 log₁₀ PFU/mL, respectively (Nguyet et al., 2013; Aubry
473 et al., 2020; Lequime et al., 2020). The CHIKV time-independent infection rate and relatively low OID_{50%} in
474 *Ae. albopictus* suggests that primary infection of midgut cells is rapid and efficient. Such CHIKV midgut
475 infection pattern could be promoted by the presence of several potential midgut receptors for *Alphavirus*
476 entry in mosquitoes (Franz et al., 2015). Importantly, a 0.5 log₁₀ FFU/mL increase in OID_{50%} during the
477 exponential phase results in twice as much infected mosquitoes, which could exacerbate outbreaks,
478 notably upon large vector densities. Therefore, dose-response experiments at a small dose range for each
479 virus and mosquito genotype of interest would significantly improve our understanding of vector
480 competence.

481 According to our results, CHIKV dissemination from the *Ae. albopictus* midgut depends on the
482 interaction between time post-exposure and virus dose. A previous study showed that at day 6 post-
483 exposure, CHIKV dissemination rate in *Ae. albopictus* increases with virus dose, being ~10%, ~50% and
484 >80% upon 3.6, 4.4 and 5.2 log₁₀ PFU/mL in the blood meal respectively (Pesko et al., 2009). Here, we show
485 that if at least 6 days are needed to reach ~30 % dissemination upon 3.94 log₁₀ FFU/mL, virus doses of 6.07
486 and 8.63 log₁₀ FFU/mL led overall to ~90 % dissemination regardless of the time point (except at day 2 for
487 the 6.07 log₁₀ FFU/mL dose where only 40 % dissemination was observed). Of note, CHIKV dissemination
488 rate at 3.94 log₁₀ FFU/mL shall be interpreted with caution due to the low sample size that arise directly
489 from the low infection rate (1.9 to 6.5%, n = 37 to 53 individuals per time point). These results reveal the
490 ability of CHIKV to efficiently disseminate from the midgut, as modelling for a larger dose range estimates
491 that all infected mosquitoes eventually disseminate even at the lowest dose considered (2 log₁₀ FFU/mL).
492 CHIKV and ZIKV present a nearly identical OID_{50%} suggesting similar midgut infection potential in *Ae.*
493 *albopictus*. However, ZIKV dissemination is slower and, to a minor extent, reaches lower value compared
494 to CHIKV (Lequime et al., 2020). This discrepancy might be due to viral replication in the midgut as
495 dissemination rate correlates with midgut viral load (Houk et al., 1981; Bosio et al., 1998; Dickson et al.,
496 2014; Vazeille et al., 2019; Carpenter et al., 2021). CHIKV dissemination might arise from an efficient
497 replication in the midgut tissue. Recently, the CHIKV 3' untranslated region was recently shown to promote
498 dissemination through an increased viral replication in the mosquito midgut (Merwaiss et al., 2020).

499 Ultimately, arboviruses infect and replicate in mosquito salivary glands, this step being essential to
500 allow virus transmission to the host (Vega-Rúa et al., 2015; Raquin & Lambrechts, 2017). Virus prevalence
501 in the head is often used as a proxy for transmission potential but it is likely an overestimate due to salivary
502 glands barriers, notably for CHIKV (Sanchez-Vargas et al., 2021). Our study shows that ~60 % of the
503 mosquitoes with disseminated infection eventually become infectious, this being an underestimate of
504 mosquito-to-host transmission potential due to the use of forced salivation technique (Gloria-Soria et al.,
505 2022). Moreover, transmission rate strongly depends on the time post-exposure. Previously, the time to
506 reach 50 % of infectious mosquitoes in the population (EIP_{50%}) was estimated by a meta-analysis at 7 days
507 (± 1 day), based on dissemination data and for mosquitoes exposed to relatively high virus doses

508 (Christofferson et al., 2014). Despite no overall effect of virus dose on the transmission rate ($P_{\text{dose}} = 0.18$),
509 CHIKV EIP_{50%} was 7.5 and 3.5 days in mosquitoes exposed to 5.68 or 8.06 log₁₀ FFU/mL, respectively,
510 suggesting that virus dose might influence CHIKV transmission. Increasing sample size and/or testing an
511 intermediate virus dose (e.g. 6 log₁₀ FFU/mL) could help to better capture the impact of virus dose on
512 transmission rate and resolve this discrepancy. Interestingly, when considering all CHIKV-positive salivas
513 (including the ones with only CHIKV RNA but found negative during infectious titration), the CHIKV RNA
514 load in the saliva depends on time post-exposure and virus dose but not in interaction. Overall, the CHIKV
515 load in saliva seems higher at high dose but decreases overtime, questioning arbovirus-salivary glands
516 interaction. In a previous study, individual ZIKV-disseminated *Ae. aegypti* mosquitoes were offered
517 successive non-infectious blood meals in an attempt to monitor expelled virus during feeding in a non-
518 sacrificial manner. Authors observed an on/off presence of ZIKV in the blood meal for a single individual
519 over time; however, whether this is due to biological or methodological causes is unclear (Mayton et al.,
520 2021). In *Ae. albopictus*, up to 10,000-fold difference of CHIKV RNA load in the saliva was found between
521 individuals at a given time point and dose, in accordance with previous results (Dubrulle et al., 2009; Bohers
522 et al., 2020; Robison et al., 2020). No correlation was found between CHIKV titer in the salivary glands and
523 in the saliva, that might be linked with such inter-individual variations (Sanchez-Vargas et al., 2019). Despite
524 several studies that identified histological and genetical factors modulating viral infection in this tissue, it
525 is still unclear how and in which amount infectious virions are produced in salivary glands and then
526 transferred into the saliva over time (Ciano et al., 2014; Modahl et al., 2019; Chowdhury et al., 2021;
527 Sanchez-Vargas et al., 2021). Notably, viral particles in the saliva might use specific viral factors and/or
528 mosquito saliva proteins to persist in the saliva and promote their transmission (Pompon et al., 2017;
529 Marin-Lopez et al., 2021). This is key as virus titer in the mosquito inoculum is associated with viraemia
530 level and symptoms severity in mice and macaques models (Labadie et al., 2010; Zhang et al., 2022).

531

532 Genetic and environmental factors impacting intra-vector dynamics

533 VComp is a composite phenotype that also depends on the interaction between virus genotype,
534 mosquito genotype and temperature (Zouache et al., 2014). From a virus perspective, some CHIKV
535 mutations that impact VComp were already described and could be useful for epidemiological monitoring,
536 even if data suggest that overall CHIKV swarm maintains an intermediate mutation frequency to avoid
537 fitness loss in the mosquito (Coffey et al., 2014). Transcriptomics and quantitative genetics studies led to
538 the identification of mosquito genetic loci that constitute interesting targets towards engineered vector
539 control approaches, as shown for *Flaviviridae* (Bosio et al., 2000; Raquin et al., 2017; Aubry et al., 2020;
540 Merklung et al., 2020; Williams et al., 2020; Dong et al., 2022). In addition, mosquitoes host a microbiota
541 composed of bacteria, viruses, fungi and protists that have a major impact on vector's biology (Guégan
542 et al., 2018). Some of these micro-organisms are associated with a decrease in arbovirus transmission and
543 constitute interesting vector control tools, like *Wolbachia* or *Delftia tsuruhatensis* bacteria blocking DENV
544 and *Plasmodium* infection, respectively or insect-specific viruses modulating *Ae. aegypti* vector
545 competence for DENV (Olmo et al., 2018; 2023; Huang et al., 2023). Despite an antiviral activity of
546 *Wolbachia* against CHIKV in *Ae. aegypti*, as well as in *Ae. albopictus* C6/36 cell line, no CHIKV blocking was
547 detected in *Ae. albopictus* mosquitoes (Mousson et al., 2012; Raquin et al., 2015; Aliota et al., 2016).
548 Moreover, *Ae. albopictus* infection by CHIKV impacts mosquito bacterial community composition while
549 several *Ae. albopictus* symbionts were associated with an increase of CHIKV infection (Zouache et al., 2012;
550 Monteiro et al., 2019). The reason for this lack of microbiota-mediated antiviral blocking against CHIKV in
551 *Ae. albopictus* remains obscure, but could depend on mosquito and virus genotype and/or temperature as
552 *Ae. albopictus* microbiota composition depends on the temperature (Bellone et al., 2023). This interaction
553 should be further studied as it could impact arbovirus transmission, as suggested by models estimating
554 that the release of *Wolbachia*-infected *Ae. aegypti* against DENV will be less efficient upon long heatwaves
555 due to loss of *Wolbachia* infection upon high temperatures (Vásquez et al., 2023). With the exception of
556 DENV genotype (Fontaine et al., 2018), the impact of aforementioned factors was not tested on VComp
557 dynamics and it will be interesting to determine if these factors, beyond modulating VComp at discrete
558 time, impact the proportion of infectious mosquitoes over time.

559

560 Human viremia and infectiousness to mosquitoes

561 A large majority of VComp studies exposed *Ae. albopictus* to a high ($>7 \log_{10}$ plaque-forming units
562 (PFU)/mL) CHIKV titer in the blood meal (Coffey et al., 2014). According to our estimate, CHIKV viraemia in
563 humans can reach $>7 \log_{10}$ PFU equivalent per mL of blood, although this corresponds to the highest value
564 measured within a short time window (<2 days). Our CHIKV viraemia estimate from human longitudinal
565 data lasts from 4 to 12 days with a mean maximum titer of $7.55 \log_{10}$ PFU/mL, which is largely supported
566 by previous human and nonhuman studies (Lanciotti et al., 2007; Panning et al., 2008; Labadie et al., 2010;
567 Schwartz & Albert, 2010). The mean human viraemia is above $3.94 \log_{10}$ FFU/mL during 5.5 days, implying
568 that humans are infectious to mosquitoes during more than half of their viraemia. These data are key to
569 improve sanitary guidelines for the management of CHIKV infections and spread. However, major
570 differences in CHIKV viraemia magnitude and length are observed between individual hosts, which can be
571 associated with host and/or virus genotypes as observed in dengue virus (DENV)-infected patients (Nguyet
572 et al., 2013). In addition, if artificial mosquito blood feeding limits variation in blood composition and
573 promotes reproducibility, it does not necessary represent the native infectiousness of human-derived
574 arbovirus for mosquitoes. This is partly linked to host plasma factors level (IgM, IgG, low-density
575 lipoproteins or gamma-aminobutyric acid) while asymptomatic DENV cases are more infectious to
576 mosquitoes than symptomatic counterparts at a given dose suggesting a link between host immune
577 response and vector transmission (Nguyet et al., 2013; Duong et al., 2015; Wagar et al., 2017; Zhu et al.,
578 2017). Moreover, for CHIKV, $\sim 85\%$ infections are symptomatic with a median blood titer about 100-fold
579 higher compare to asymptomatic carriers, although this difference was not statistically significant
580 (Appassakij et al., 2013). Thus, improving epidemiological models by implementing the time-dependant
581 human host infectiousness to mosquitoes represents an interesting lead to better anticipate and prevent
582 CHIKV outbreaks. This notably prompts the need for viraemia monitoring over time in large groups of
583 patients infected by arboviruses, using standardized virus titration procedures to facilitate comparisons
584 and calibrate dose-response experiments in mosquitoes. This also requires other improvements of
585 modelling strategies to account for mosquito and human populations structure, sanitary measures as well
586 as *Ae. albopictus* tendency to take several consecutive blood meals. Indeed, virus dissemination increases
587 with gonotrophic cycles and that successive bloodmeals are associated with a shortened EIP (Delatte et al.,
588 2010; Armstrong et al., 2019; Fikrig & Harrington, 2021; Mulatier et al., 2023). Although those limitations
589 could modulate the explosiveness of the outbreak and could be improved, our data support that CHIKV
590 transmission potential of local *Ae. albopictus* is not a limiting factor for local CHIKV emergence and spread.
591 Finally, such a standardized experimental design can be used to investigate the impact of additional
592 (a)biotic factors on VComp dynamics.

593 Beyond virus dose and time post virus exposure, mosquito and virus genotype, mosquito microbiota
594 and temperature are currently identified as major VComp drivers. Therefore, locally-acquired VComp data
595 from area at risk for arbovirus circulation are needed. This could be achieved by exposing autochthonous
596 field-derived mosquito populations to virus strains currently circulating (or at risk of introduction) upon a
597 range of virus dose and temperature spanning the human viremia and the mosquito season, respectively,
598 while controlling experimentally mosquito microbiota. This is unlikely to be done within a single
599 experiment but will require the incremental acquisition of data sets for each factor, underlying the
600 importance of experimental procedure standardization. Interestingly, modelisation of VComp based on
601 available data could help to target a range of the factor's values to be tested experimentally, as exemplified
602 with temperature (Shocket et al., 2020). These factors act together in interaction making difficult to
603 dissociate their real impact on VComp in the field. Deciphering the complex interplay between each factor
604 on VComp is challenging but feasible (Audsley et al., 2017) and holistic interaction studies could help to
605 address this issue experimentally (Brinker et al., 2019). Beyond experimental conditions, our work
606 underlines that monitoring intra-vector dynamics rather than end-point VComp is key to accurately
607 quantify VComp variations and better estimate VCap (Christofferson & Mores, 2011). Several studies
608 estimated VCap through the lens of mosquito density upon environmental variations (e.g. temperature,
609 micro-climate, land cover) but with limited ecological (mosquito survival rate, biting rate, density per host)
610 and VComp data, notably regarding intra-vector dynamics (Murdock et al., 2017; Wimberly et al., 2020;
611 Peña-García et al., 2023). This highlights the current need for additional VComp and VCap-related studies
612 using field-derived material, as well as increasing efforts between vector biology and modeling fields
613 towards an integrative VCap estimation notably regarding intra-vector arbovirus dynamics. Altogether, this
614 will improve vector control strategies and case management by health authorities.

615

616

Appendices

617 FigS1 - CHIKV infectious titer is stable upon a one hour incubation at 37°C in human erythrocytes
618 suspension. Refers to raw data table “blood_titration_FFU.txt” (see data availability section).

619 FigS2 - Rescaled mosquito transmission dynamics. Refers to raw data table
620 “Data_titer_EIPdyna_final.txt” (see data availability section).

621 FigS3 - Time-course of CHIKV load in mosquito saliva. Refers to raw data table
622 “Data_CHIKV_RNA_load_saliva.txt” (see data availability section).

623 TabS1 - Proportion of infected, disseminated and infectious mosquitoes over time according to the
624 dose of CHIKV in the blood meal. Refers to raw data table “Raw_data_viginier_et_al2023” (see data
625 availability section).

626

627

Acknowledgements

628 This project was funded by the scientific breakthrough project Micro-Be-Have (Microbial impact on
629 insect behavior) of the Université de Lyon within the program Investissements d’Avenir (ANR-11-IDEX-
630 0007; ANR-16-IDEX-0005). We thank the Equipex InfectioTron program and its project manager Isabelle
631 Weiss. We also thank all the members of the Micro-Be-Have consortium for insightful discussions. We
632 thank Anna-Bella Failloux and Patrick Mavingui for the CHIKV 06.21 isolate. We acknowledge the
633 contribution of SFR Biosciences (UAR3444/CNRS, US8/Inserm, ENS de Lyon, Université Claude Bernard Lyon
634 1) AniRa biosafety level 3 platform (Marie-Pierre Confort) and plateau Analyse Génétique et Cellulaire
635 (Bariza Blanquier) facilities in Lyon. We also thank 2 anonymous reviewers for helpful comments on a
636 previous version of this manuscript.

637

638

Data, scripts, code, and supplementary information availability

639 Data, R scripts, supplementary information and main figures in full size are available online:
640 <https://doi.org/10.5281/zenodo.8033668>

641

Conflict of interest disclosure

642 The authors declare that they comply with the PCI rule of having no financial conflicts of interest in
643 relation to the content of the article.

644 Sebastian Lequime is a recommender for PCI infections.

645

Author contributions

646 **BV:** Investigation; Data curation; Validation

647 **LC:** Investigation; Data curation; Validation

648 **CG:** Investigation; Data curation; Validation

649 **EM:** Resources

650 **CM:** Resources

651 **CVM:** Funding acquisition; Resources; Supervision; Writing – review and editing

652 **GM:** Funding acquisition; Writing – review and editing

653 **AF:** Data curation; Formal analysis; Software; Visualization; Methodology; Writing – review and editing

654 **SL:** Data curation; Formal analysis; Software; Visualization; Methodology; Writing – review and editing

655 **MR:** Funding acquisition; Supervision; Writing – review and editing

656 **FA:** Funding acquisition; Project administration; Supervision; Writing – review and editing

657 **VR:** Conceptualization; Investigation; Formal analysis; Data curation; Methodology; Investigation; Project
658 administration; Supervision; Validation; Visualization; Writing – original draft; Writing – review and
659 editing.

660 **Funding**

661 Micro-Be-Have (Microbial impact on insect behavior) of the Université de Lyon within the program
662 Investissements d’Avenir (ANR-11-IDEX-0007; ANR-16-IDEX-0005).

663 **References**

664 Aliota MT, Walker EC, Yepes AU, Velez ID, Christensen BM, Osorio JE (2016) The wMel Strain of *Wolbachia*
665 Reduces Transmission of Chikungunya Virus in *Aedes aegypti*. *PLoS neglected tropical diseases*, **10**,
666 e0004677. <https://doi.org/10.1371/journal.pntd.0004677>

667 Appassakij H, Khuntikij P, Kemapunmanus M, Wutthanarungsan R, Silpapojakul K (2013) Viremic profiles
668 in CHIKV-infected cases. *Transfusion*, **53**, 2567–2574. [https://doi.org/10.1111/j.1537-
669 2995.2012.03960.x](https://doi.org/10.1111/j.1537-2995.2012.03960.x)

670 Armstrong PM, Ehrlich HY, Magalhaes T, Miller MR, Conway PJ, Bransfield A, Misencik MJ, Gloria-Soria A,
671 Warren JL, Andreadis TG, Shepard JJ, Foy BD, Pitzer VE, Brackney DE (2019) Successive blood meals
672 enhance virus dissemination within mosquitoes and increase transmission potential. *Nature*
673 *microbiology*, 1–9. <https://doi.org/10.1038/s41564-019-0619-y>

674 Aubry F, Dabo S, Manet C, Filipović I, Rose NH, Miot EF, Martynow D, Baidaliuk A, Merklings SH, Dickson
675 LB, Crist AB, Anyango VO, Romero-Vivas CM, Vega-Rúa A, Dusfour I, Jiolle D, Paupy C, Mayanja MN,
676 Lutwama JJ, Kohl A, Duong V, Ponlawat A, Sylla M, Akorli J, Otoo S, Lutomiah J, Sang R, Mutebi J-P,
677 Cao-Lormeau V-M, Jarman RG, Diagne CT, Faye O, Faye O, Sall AA, McBride CS, Montagutelli X, Rašić
678 G, Lambrechts L (2020) Enhanced Zika virus susceptibility of globally invasive *Aedes aegypti*
679 populations. *Science*, **370**, 991–996. <https://doi.org/10.1126/science.abd3663>

680 Audsley MD, Ye YH, McGraw EA (2017) The microbiome composition of *Aedes aegypti* is not critical for
681 *Wolbachia*-mediated inhibition of dengue virus. *PLoS Neglected Tropical Diseases*, **11**, e0005426.
682 <https://doi.org/10.1371/journal.pntd.0005426>

683 Bellone R, Lechat P, Mousson L, Gilbert V, Piorkowski G, Bohers C, Merits A, Kornobis E, Reveillaud J,
684 Paupy C, Vazeille M, Martinet J-P, Madec Y, Lamballerie XD, Dauga C, Failloux A-B (2023) Climate
685 change and vector-borne diseases: a multi-omics approach of temperature-induced changes in the
686 mosquito. *Journal of Travel Medicine*, **30**. <https://doi.org/10.1093/jtm/taad062>

687 Bhatt S, Gething PW, Brady OJ, Messina JP, Farlow AW, Moyes CL, Drake JM, Brownstein JS, Hoen AG,
688 Sankoh O, Myers MF, George DB, Jaenisch T, Wint GRW, Simmons CP, Scott TW, Farrar JJ, Hay SI
689 (2013) The global distribution and burden of dengue. *Nature*, **496**, 504–507.
690 <https://doi.org/10.1038/nature12060>

691 Bohers C, Mousson L, Madec Y, Vazeille M, Rhim A, M’ghirbi Y, Bouattour A, Failloux A-B (2020) The
692 recently introduced *Aedes albopictus* in Tunisia has the potential to transmit chikungunya, dengue
693 and Zika viruses. *PLoS Neglected Tropical Diseases*, **14**, e0008475.
694 <https://doi.org/10.1371/journal.pntd.0008475>

- 695 Bonilauri P, Bellini R, Calzolari M, Angelini R, Venturi L, Fallacara F, Cordioli P, Angelini P, Venturelli C,
696 Merialdi G, Dottori M (2008) Chikungunya Virus in *Aedes albopictus*, Italy. *Emerging Infectious*
697 *Diseases*, **14**, 852–854. <https://doi.org/10.3201/eid1405.071144>
- 698 Bosio CF, Beaty BJ, Black WC (1998) Quantitative genetics of vector competence for dengue-2 virus in
699 *Aedes aegypti*. *The American Journal of Tropical Medicine and Hygiene*, **59**, 965–970.
700 <https://doi.org/10.4269/ajtmh.1998.59.965>
- 701 Bosio CF, Fulton RE, Salasek ML, Beaty BJ, Black WC (2000) Quantitative trait loci that control vector
702 competence for dengue-2 virus in the mosquito *Aedes aegypti*. *Genetics*, **156**, 687–698.
703 <https://doi.org/10.1093/genetics/156.2.687>
- 704 Brinker P, Fontaine MC, Beukeboom LW, Salles JF (2019) Host, Symbionts, and the Microbiome: The
705 Missing Tripartite Interaction. *Trends in Microbiology*, **27**, 480–488.
706 <https://doi.org/10.1016/j.tim.2019.02.002>
- 707 Carpenter A, Bryant WB, Santos SR, Clem RJ (2021) Infection of *Aedes aegypti* Mosquitoes with Midgut-
708 Attenuated Sindbis Virus Reduces, but Does Not Eliminate, Disseminated Infection. *Journal of*
709 *Virology*, **95**, e00136-21. <https://doi.org/10.1128/jvi.00136-21>
- 710 Chowdhury A, Modahl CM, Missé D, Kini RM, Pompon J (2021) High resolution proteomics of *Aedes*
711 *aegypti* salivary glands infected with either dengue, Zika or chikungunya viruses identify new virus
712 specific and broad antiviral factors. *Scientific Reports*, **11**, 23696. [https://doi.org/10.1038/s41598-](https://doi.org/10.1038/s41598-021-03211-0)
713 [021-03211-0](https://doi.org/10.1038/s41598-021-03211-0)
- 714 Christofferson RC, Chisenhall DM, Wearing HJ, Mores CN (2014) Chikungunya Viral Fitness Measures
715 within the Vector and Subsequent Transmission Potential. *PLoS ONE*, **9**, e110538.
716 <https://doi.org/10.1371/journal.pone.0110538>
- 717 Christofferson RC, Mores CN (2011) Estimating the Magnitude and Direction of Altered Arbovirus
718 Transmission Due to Viral Phenotype. *PLoS ONE*, **6**, e16298.
719 <https://doi.org/10.1371/journal.pone.0016298>
- 720 Ciano K, Saredy J, Bowers D (2014) Heparan Sulfate Proteoglycan: An Arbovirus Attachment Factor
721 Integral to Mosquito Salivary Gland Ducts. *Viruses*, **6**, 5182–5197. <https://doi.org/10.3390/v6125182>
- 722 Coffey LL, Failloux A-B, Weaver SC (2014) Chikungunya Virus–Vector Interactions. *Viruses*, **6**, 4628–4663.
723 <https://doi.org/10.3390/v6114628>
- 724 Delatte H, Desvars A, Bouétard A, Bord S, Gimonneau G, Vourc'h G, Fontenille D (2010) Blood-Feeding
725 Behavior of *Aedes albopictus*, a Vector of Chikungunya on La Réunion. *Vector-Borne and Zoonotic*
726 *Diseases*, **10**, 249–258. <https://doi.org/10.1089/vbz.2009.0026>
- 727 Delisle E, Rousseau C, Broche B, Leparç-Goffart I, L'Ambert G, Cochet A, Prat C, Foulongne V, Ferré JB,
728 Catelinois O, Flusin O, Tchernonog E, Moussion IE, Wiegandt A, Septfons A, Mendy A, Moyano MB,
729 Laporte L, Maurel J, Jourdain F, Reynes J, Paty MC, Golliot F (2015) Chikungunya outbreak in
730 Montpellier, France, September to October 2014. *Eurosurveillance*, **20**. [https://doi.org/10.2807/1560-](https://doi.org/10.2807/1560-7917.es2015.20.17.21108)
731 [7917.es2015.20.17.21108](https://doi.org/10.2807/1560-7917.es2015.20.17.21108)
- 732 Dickson LB, Sanchez-Vargas I, Sylla M, Fleming K, Black WC (2014) Vector competence in West African
733 *Aedes aegypti* Is Flavivirus species and genotype dependent. *PLoS neglected tropical diseases*, **8**,
734 e3153. <https://doi.org/10.1371/journal.pntd.0003153>

- 735 Dong Y, Dong S, Dizaji NB, Rutkowski N, Pohlenz T, Myles K, Dimopoulos G (2022) The *Aedes aegypti*
736 siRNA pathway mediates broad-spectrum defense against human pathogenic viruses and modulates
737 antibacterial and antifungal defenses. *PLoS Biology*, **20**, e3001668.
738 <https://doi.org/10.1371/journal.pbio.3001668>
- 739 Dubrulle M, Mousson L, Moutailler S, Vazeille M, Failloux A-B (2009) Chikungunya virus and *Aedes*
740 mosquitoes: saliva is infectious as soon as two days after oral infection. *PLoS One*, **4**, e5895.
741 <https://doi.org/10.1371/journal.pone.0005895>
- 742 Duong V, Lambrechts L, Paul RE, Ly S, Lay RS, Long KC, Huy R, Tarantola A, Scott TW, Sakuntabhai A,
743 Buchy P (2015) Asymptomatic humans transmit dengue virus to mosquitoes. *Proceedings of the*
744 *National Academy of Sciences*, **112**, 14688–14693. <https://doi.org/10.1073/pnas.1508114112>
- 745 Favier C, Schmit D, Mller-Graf CDM, Cazelles B, Degallier N, Mondet B, Dubois MA (2005) Influence of
746 spatial heterogeneity on an emerging infectious disease: the case of dengue epidemics. *Proceedings*
747 *of the Royal Society B: Biological Sciences*, **272**, 1171–1177. <https://doi.org/10.1098/rspb.2004.3020>
- 748 Fikrig K, Harrington LC (2021) Understanding and interpreting mosquito blood feeding studies: the case of
749 *Aedes albopictus*. *Trends in Parasitology*, **37**, 959–975. <https://doi.org/10.1016/j.pt.2021.07.013>
- 750 Fontaine A, Lequime S, Moltini-Conclois I, Jiolle D, Leparç-Goffart I, Reiner RC, Lambrechts L (2018)
751 Epidemiological significance of dengue virus genetic variation in mosquito infection dynamics. *PLoS*
752 *Pathogens*, **14**, e1007187. <https://doi.org/10.1371/journal.ppat.1007187>
- 753 Franke F, Giron S, Cochet A, Jeannin C, Leparç-Goffart I, Valk H de, Jourdain F, Lamballerie X de, L'Ambert
754 G, Paty MC (2019) Autochthonous chikungunya and dengue fever outbreak in Mainland France, 2010-
755 2018. *European Journal of Public Health*, **29**. <https://doi.org/10.1093/eurpub/ckz186.628>
- 756 Franz AWE, Kantor AM, Passarelli AL, Clem RJ (2015) Tissue Barriers to Arbovirus Infection in Mosquitoes.
757 *Viruses*, **7**, 3741–3767. <https://doi.org/10.3390/v7072795>
- 758 Gloria-Soria A, Brackney DE, Armstrong PM (2022) Saliva collection via capillary method may
759 underestimate arboviral transmission by mosquitoes. *Parasites & Vectors*, **15**, 103.
760 <https://doi.org/10.1186/s13071-022-05198-7>
- 761 Gloria-Soria A, Payne AF, Bialosuknia SM, Stout J, Mathias N, Eastwood G, Ciota AT, Kramer LD,
762 Armstrong PM (2020) Vector Competence of *Aedes albopictus* Populations from the Northeastern
763 United States for Chikungunya, Dengue, and Zika Viruses. *The American Journal of Tropical Medicine*
764 *and Hygiene*. <https://doi.org/10.4269/ajtmh.20-0874>
- 765 Gratz NG (2004) Critical review of the vector status of *Aedes albopictus*. *Medical and Veterinary*
766 *Entomology*, **18**, 215–227. <https://doi.org/10.1111/j.0269-283x.2004.00513.x>
- 767 Greiser-Wilke I, Moennig V, Kaaden O-R, Figueiredo LTM (1989) Most Alphaviruses Share a Conserved
768 Epitopic Region on Their Nucleocapsid Protein. *Journal of General Virology*, **70**, 743–748.
769 <https://doi.org/10.1099/0022-1317-70-3-743>
- 770 Guégan M, Zouache K, Démichel C, Minard G, Van VT, Potier P, Mavingui P, Moro CV (2018) The mosquito
771 holobiont: fresh insight into mosquito-microbiota interactions. *Microbiome*, **6**, 49.
772 <https://doi.org/10.1186/s40168-018-0435-2>

- 773 Heitmann A, Jansen S, Lühken R, Leggewie M, Schmidt-Chanasit J, Tannich E (2018) Forced Salivation As a
774 Method to Analyze Vector Competence of Mosquitoes. *Journal of Visualized Experiments : JoVE*,
775 57980. <https://doi.org/10.3791/57980>
- 776 Houk EJ, Hardy JL, Presser SB, Kramer LD (1981) Dissemination Barriers for Western Equine
777 Encephalomyelitis Virus in *Culex tarsalis* Infected after Ingestion of Low Viral Doses. *The American*
778 *Journal of Tropical Medicine and Hygiene*, **30**, 190–197. <https://doi.org/10.4269/ajtmh.1981.30.190>
- 779 Huang W, Rodrigues J, Bilgo E, Tormo JR, Challenger JD, Cozar-Gallardo CD, Pérez-Victoria I, Reyes F,
780 Castañeda-Casado P, Gnambani EJ, Hien DF de S, Konkobo M, Urones B, Coppens I, Mendoza-Losana
781 A, Ballell L, Diabate A, Churcher TS, Jacobs-Lorena M (2023) *Delftia tsuruhatensis* TC1 symbiont
782 suppresses malaria transmission by anopheline mosquitoes. *Science*, **381**, 533–540.
783 <https://doi.org/10.1126/science.adf8141>
- 784 Hurk AF van den, Hall-Mendelin S, Pyke AT, Smith GA, Mackenzie JS (2010) Vector Competence of
785 Australian Mosquitoes for Chikungunya Virus. *Vector-Borne and Zoonotic Diseases*, **10**, 489–495.
786 <https://doi.org/10.1089/vbz.2009.0106>
- 787 Islam ZU, Bishop SC, Savill NJ, Rowland RRR, Lunney JK, Tribble B, Doeschl-Wilson AB (2013) Quantitative
788 Analysis of Porcine Reproductive and Respiratory Syndrome (PRRS) Viremia Profiles from
789 Experimental Infection: A Statistical Modelling Approach. *PLoS ONE*, **8**, e83567.
790 <https://doi.org/10.1371/journal.pone.0083567>
- 791 Labadie K, Larcher T, Joubert C, Mannioui A, Delache B, Brochard P, Guigand L, Dubreil L, Lebon P, Verrier
792 B, Lamballerie X de, Suhrbier A, Cherel Y, Grand RL, Roques P (2010) Chikungunya disease in
793 nonhuman primates involves long-term viral persistence in macrophages. *Journal of Clinical*
794 *Investigation*, **120**, 894–906. <https://doi.org/10.1172/jci40104>
- 795 Labeaud AD, Bashir F, King CH (2011) Measuring the burden of arboviral diseases: the spectrum of
796 morbidity and mortality from four prevalent infections. *Population Health Metrics*, **9**, 1.
797 <https://doi.org/10.1186/1478-7954-9-1>
- 798 Lanciotti RS, Kosoy OL, Laven JJ, Panella AJ, Velez JO, Lambert AJ, Campbell GL (2007) Chikungunya virus
799 in US travelers returning from India, 2006. *Emerging Infectious Diseases*, **13**, 764–767.
800 <https://doi.org/10.3201/eid1305.070015>
- 801 Lequime S, Bastide P, Dellicour S, Lemey P, Baele G (2020) nosoi: A stochastic agent-based transmission
802 chain simulation framework in r. *Methods in Ecology and Evolution*, **11**, 1002–1007.
803 <https://doi.org/10.1111/2041-210x.13422>
- 804 Lequime S, Dehecq J-S, Matheus S, Laval F de, Almeras L, Briolant S, Fontaine A (2020) Modeling intra-
805 mosquito dynamics of Zika virus and its dose-dependence confirms the low epidemic potential of
806 *Aedes albopictus*. *PLOS Pathogens*, **16**, e1009068. <https://doi.org/10.1371/journal.ppat.1009068>
- 807 Mariconti M, Obadia T, Mousson L, Malacrida A, Gasperi G, Failloux A-B, Yen P-S (2019) Estimating the
808 risk of arbovirus transmission in Southern Europe using vector competence data. *Scientific Reports*, **9**,
809 17852. <https://doi.org/10.1038/s41598-019-54395-5>
- 810 Marin-Lopez A, Jiang J, Wang Y, Cao Y, MacNeil T, Hastings AK, Fikrig E (2021) *Aedes aegypti* SNAP and a
811 calcium transporter ATPase influence dengue virus dissemination. *PLoS Neglected Tropical Diseases*,
812 **15**, e0009442. <https://doi.org/10.1371/journal.pntd.0009442>

- 813 Mayton EH, Hernandez HM, Vitek CJ, Christofferson RC (2021) A Method for Repeated, Longitudinal
814 Sampling of Individual *Aedes aegypti* for Transmission Potential of Arboviruses. *Insects*, **12**, 292.
815 <https://doi.org/10.3390/insects12040292>
- 816 Merklings SH, Raquin V, Dabo S, Henrion-Lacritick A, Blanc H, Moltini-Conclois I, Frangeul L, Varet H, Saleh
817 M-C, Lambrechts L (2020) Tudor-SN Promotes Early Replication of Dengue Virus in the *Aedes aegypti*
818 Midgut. *iScience*, **23**, 100870. <https://doi.org/10.1016/j.isci.2020.100870>
- 819 Merwaiss F, Filomatori CV, Susuki Y, Bardossy ES, Alvarez DE, Saleh M-C (2020) Chikungunya virus
820 replication rate determines the capacity of crossing tissue barriers in mosquitoes. *Journal of Virology*,
821 **95**. <https://doi.org/10.1128/jvi.01956-20>
- 822 Modahl C, Chowdhury A, Oliveira F, Kini RM, Pompon J (2019) Salivary gland RNA-seq from arbovirus-
823 infected *Aedes aegypti* and *Aedes albopictus* provides insights into virus transmission. *Access*
824 *Microbiology*, **1**. <https://doi.org/10.1099/acmi.imav2019.po0039>
- 825 Moloney RM, Kmush B, Rudolph KE, Cummings DAT, Lessler J (2014) Incubation Periods of Mosquito-
826 Borne Viral Infections: A Systematic Review. *The American Journal of Tropical Medicine and Hygiene*,
827 **90**, 882–891. <https://doi.org/10.4269/ajtmh.13-0403>
- 828 Mombouli J-V, Bitsindou P, Elion DOA, Grolla A, Feldmann H, Niama FR, Parra H-J, Munster VJ (2013)
829 Chikungunya Virus Infection, Brazzaville, Republic of Congo, 2011. *Emerging Infectious Diseases*, **19**,
830 1542–1543. <https://doi.org/10.3201/eid1909.130451>
- 831 Monteiro VVS, Navegantes-Lima KC, Lemos AB de, Silva GL da, Gomes R de S, Reis JF, Junior LCR, Silva OS
832 da, Romão PRT, Monteiro MC (2019) *Aedes*–Chikungunya Virus Interaction: Key Role of Vector
833 Midguts Microbiota and Its Saliva in the Host Infection. *Frontiers in Microbiology*, **10**, 492.
834 <https://doi.org/10.3389/fmicb.2019.00492>
- 835 Mousson L, Zouache K, Arias-Goeta C, Raquin V, Mavingui P, Failloux A-B (2012) The native *Wolbachia*
836 symbionts limit transmission of dengue virus in *Aedes albopictus*. *PLoS neglected tropical diseases*, **6**,
837 e1989. <https://doi.org/10.1371/journal.pntd.0001989>
- 838 Moutailler S, Barré H, Vazeille M, Failloux A (2009) Recently introduced *Aedes albopictus* in Corsica is
839 competent to Chikungunya virus and in a lesser extent to dengue virus. *Tropical Medicine &*
840 *International Health*, **14**, 1105–1109. <https://doi.org/10.1111/j.1365-3156.2009.02320.x>
- 841 Mulatier M, Boullis A, Dollin C, Cebrián-Torrejón G, Vega-Rúa A (2023) Chikungunya Virus Infection and
842 Gonotrophic Cycle Shape *Aedes aegypti* Oviposition Behavior and Preferences. *Viruses*, **15**, 1043.
843 <https://doi.org/10.3390/v15051043>
- 844 Murdock CC, Evans MV, McClanahan TD, Miazgowicz KL, Tesla B (2017) Fine-scale variation in
845 microclimate across an urban landscape shapes variation in mosquito population dynamics and the
846 potential of *Aedes albopictus* to transmit arboviral disease. *PLoS Neglected Tropical Diseases*, **11**,
847 e0005640. <https://doi.org/10.1371/journal.pntd.0005640>
- 848 Nguyet MN, Duong THK, Trung VT, Nguyen THQ, Tran CNB, Long VT, Dui LT, Nguyen HL, Farrar JJ, Holmes
849 EC, Rabaa MA, Bryant JE, Nguyen TT, Nguyen HTC, Nguyen LTH, Pham MP, Nguyen HT, Luong TTH,
850 Wills B, Nguyen CVV, Wolbers M, Simmons CP (2013) Host and viral features of human dengue cases
851 shape the population of infected and infectious *Aedes aegypti* mosquitoes. *Proceedings of the*
852 *National Academy of Sciences of the United States of America*, **110**, 9072–9077.
853 <https://doi.org/10.1073/pnas.1303395110>

- 854 Olmo RP, Ferreira AGA, Izidoro-Toledo TC, Aguiar ERGR, Faria IJS de, Souza KPR de, Osório KP, Kuhn L,
855 Hammann P, Andrade EG de, Todjro YM, Rocha MN, Leite THJF, Amadou SCG, Armache JN, Paro S,
856 Oliveira CD de, Carvalho FD, Moreira LA, Marois E, Imler J-L, Marques JT (2018) Control of dengue
857 virus in the midgut of *Aedes aegypti* by ectopic expression of the dsRNA-binding protein Loqs2.
858 *Nature Microbiology*, **3**, 1385–1393. <https://doi.org/10.1038/s41564-018-0268-6>
- 859 Olmo RP, Todjro YMH, Aguiar ERGR, Almeida JPP de, Ferreira FV, Armache JN, Faria IJS de, Ferreira AGA,
860 Amadou SCG, Silva ATS, Souza KPR de, Vilela APP, Babarit A, Tan CH, Diallo M, Gaye A, Paupy C,
861 Obame-Nkoghe J, Visser TM, Koenraad CJM, Wongsokarijo MA, Cruz ALC, Prieto MT, Parra MCP,
862 Nogueira ML, Avelino-Silva V, Mota RN, Borges MAZ, Drumond BP, Kroon EG, Recker M, Sedda L,
863 Marois E, Imler J-L, Marques JT (2023) Mosquito vector competence for dengue is modulated by
864 insect-specific viruses. *Nature Microbiology*, **8**, 135–149. <https://doi.org/10.1038/s41564-022-01289-4>
865
- 866 Pagès F, Peyrefitte CN, Mve MT, Jarjaval F, Brisse S, Itehan I, Gravier P, Tolou H, Nkoghe D, Grandadam
867 M (2009) *Aedes albopictus* Mosquito: The Main Vector of the 2007 Chikungunya Outbreak in Gabon.
868 *PLoS ONE*, **4**, e4691. <https://doi.org/10.1371/journal.pone.0004691>
- 869 Panning M, Grywna K, Esbroeck M van, Emmerich P, Drosten C (2008) Chikungunya fever in travelers
870 returning to Europe from the Indian Ocean region, 2006. *Emerging Infectious Diseases*, **14**, 416–422.
871 <https://doi.org/10.3201/eid1403.070906>
- 872 Paupy C, Delatte H, Bagny L, Corbel V, Fontenille D (2009) *Aedes albopictus*, an arbovirus vector: from the
873 darkness to the light. *Microbes and Infection / Institut Pasteur*, **11**, 1177–1185.
874 <https://doi.org/10.1016/j.micinf.2009.05.005>
- 875 Paupy C, Kassa FK, Caron M, Nkoghé D, Leroy EM (2012) A Chikungunya Outbreak Associated with the
876 Vector *Aedes albopictus* in Remote Villages of Gabon. *Vector-Borne and Zoonotic Diseases*, **12**, 167–
877 169. <https://doi.org/10.1089/vbz.2011.0736>
- 878 Peña-García VH, Luvall JC, Christofferson RC (2023) Arbovirus Transmission Predictions Are Affected by
879 Both Temperature Data Source and Modeling Methodologies across Cities in Colombia.
880 *Microorganisms*, **11**, 1249. <https://doi.org/10.3390/microorganisms11051249>
- 881 Pesko K, Westbrook CJ, Mores CN, Lounibos LP, Reiskind MH (2009) Effects of Infectious Virus Dose and
882 Bloodmeal Delivery Method on Susceptibility of *Aedes aegypti* and *Aedes albopictus* to Chikungunya
883 Virus. *Journal of Medical Entomology*, **46**, 395–399. <https://doi.org/10.1603/033.046.0228>
- 884 Pompon J, Manuel M, Ng GK, Wong B, Shan C, Manokaran G, Soto-Acosta R, Bradrick SS, Ooi EE, Missé D,
885 Shi P-Y, Garcia-Blanco MA (2017) Dengue subgenomic flaviviral RNA disrupts immunity in mosquito
886 salivary glands to increase virus transmission. *PLoS Pathogens*, **13**, e1006535.
887 <https://doi.org/10.1371/journal.ppat.1006535>
- 888 Raquin V, Lambrechts L (2017) Dengue virus replicates and accumulates in *Aedes aegypti* salivary glands.
889 *Virology*, **507**, 75–81. <https://doi.org/10.1016/j.virol.2017.04.009>
- 890 Raquin V, Merklung SH, Gausson V, Moltini-Conclois I, Frangeul L, Varet H, Dillies M-A, Saleh M-C,
891 Lambrechts L (2017) Individual co-variation between viral RNA load and gene expression reveals novel
892 host factors during early dengue virus infection of the *Aedes aegypti* midgut. *PLoS Neglected Tropical
893 Diseases*, **11**, e0006152. <https://doi.org/10.1371/journal.pntd.0006152>

- 894 Raquin V, Moro CV, Saucereau Y, Tran F-H, Potier P, Mavingui P (2015) Native *Wolbachia* from *Aedes*
895 *albopictus* Blocks Chikungunya Virus Infection *In Cellulo*. *PLOS ONE*, **10**, e0125066.
896 <https://doi.org/10.1371/journal.pone.0125066>
- 897 RCoreTeam (2022) R Core Team (2021) R: A Language and Environment for Statistical Computing.
- 898 Riswari SF, Ma'roef CN, Djauhari H, Kosasih H, Perkasa A, Yudhaputri FA, Artika IM, Williams M, Ven A van
899 der, Myint KS, Alisjahbana B, Ledermann JP, Powers AM, Jaya UA (2015) Study of viremic profile in
900 febrile specimens of chikungunya in Bandung, Indonesia. *Journal of clinical virology : the official*
901 *publication of the Pan American Society for Clinical Virology*, **74**, 61–5.
902 <https://doi.org/10.1016/j.jcv.2015.11.017>
- 903 Robison A, Young MC, Byas AD, Rückert C, Ebel GD (2020) Comparison of Chikungunya Virus and Zika
904 Virus Replication and Transmission Dynamics in *Aedes aegypti* Mosquitoes. *The American journal of*
905 *tropical medicine and hygiene*. <https://doi.org/10.4269/ajtmh.20-0143>
- 906 Sanchez-Vargas I, Harrington LC, Black WC, Olson KE (2019) Analysis of Salivary Glands and Saliva from
907 *Aedes albopictus* and *Aedes aegypti* Infected with Chikungunya Viruses. *Insects*, **10**, 39.
908 <https://doi.org/10.3390/insects10020039>
- 909 Sanchez-Vargas I, Olson KE, Black WC (2021) The Genetic Basis for Salivary Gland Barriers to Arboviral
910 Transmission. *Insects*, **12**, 73. <https://doi.org/10.3390/insects12010073>
- 911 Schuffenecker I, Iteman I, Michault A, Murri S, Frangeul L, Vaney M-C, Lavenir R, Pardigon N, Reynes J-M,
912 Pettinelli F, Biscornet L, Diancourt L, Michel S, Duquerroy S, Guigon G, Frenkiel M-P, Bréhin A-C,
913 Cubito N, Desprès P, Kunst F, Rey FA, Zeller H, Brisse S (2006) Genome Microevolution of Chikungunya
914 Viruses Causing the Indian Ocean Outbreak. *PLoS Medicine*, **3**, e263.
915 <https://doi.org/10.1371/journal.pmed.0030263>
- 916 Schwartz O, Albert ML (2010) Biology and pathogenesis of chikungunya virus. *Nature Reviews*
917 *Microbiology*, **8**, 491–500. <https://doi.org/10.1038/nrmicro2368>
- 918 Shocket MS, Verwillow AB, Numazu MG, Slamani H, Cohen JM, Moustaid FE, Rohr J, Johnson LR,
919 Mordecai EA (2020) Transmission of West Nile and five other temperate mosquito-borne viruses
920 peaks at temperatures between 23°C and 26°C. *eLife*, **9**, e58511. <https://doi.org/10.7554/elife.58511>
- 921 Smith DL, Battle KE, Hay SI, Barker CM, Scott TW, McKenzie FE (2012) Ross, Macdonald, and a Theory for
922 the Dynamics and Control of Mosquito-Transmitted Pathogens. *PLoS Pathogens*, **8**, e1002588.
923 <https://doi.org/10.1371/journal.ppat.1002588>
- 924 Tsetsarkin KA, Vanlandingham DL, McGee CE, Higgs S (2007) A single mutation in chikungunya virus
925 affects vector specificity and epidemic potential. *PLoS pathogens*, **3**, e201.
926 <https://doi.org/10.1371/journal.ppat.0030201>
- 927 Vásquez VN, Kueppers LM, Rašić G, Marshall JM (2023) wMel replacement of dengue-competent
928 mosquitoes is robust to near-term climate change. *Nature Climate Change*, **13**, 848–855.
929 <https://doi.org/10.1038/s41558-023-01746-w>
- 930 Vazeille M, Madec Y, Mousson L, Bellone R, Barré-Cardi H, Sousa CA, Jiolle D, Yébakima A, Lamballerie X
931 de, Failloux A-B (2019) Zika virus threshold determines transmission by European *Aedes albopictus*
932 mosquitoes. *Emerging Microbes & Infections*, **8**, 1668–1678.
933 <https://doi.org/10.1080/22221751.2019.1689797>

- 934 Vazeille M, Moutailler S, Coudrier D, Rousseaux C, Khun H, Huerre M, Thiria J, Dehecq J-S, Fontenille D,
935 Schuffenecker I, Despres P, Failloux A-B (2007) Two Chikungunya Isolates from the Outbreak of La
936 Reunion (Indian Ocean) Exhibit Different Patterns of Infection in the Mosquito, *Aedes albopictus*. *PLoS*
937 *ONE*, **2**, e1168. <https://doi.org/10.1371/journal.pone.0001168>
- 938 Vega-Rúa A, Lourenço-de-Oliveira R, Mousson L, Vazeille M, Fuchs S, Yébakima A, Gustave J, Girod R,
939 Dusfour I, Leparç-Goffart I, Vanlandingham DL, Huang Y-JS, Lounibos LP, Ali SM, Nougairède A,
940 Lamballerie X de, Failloux A-B (2015) Chikungunya Virus Transmission Potential by Local *Aedes*
941 Mosquitoes in the Americas and Europe. *PLoS Neglected Tropical Diseases*, **9**, e0003780.
942 <https://doi.org/10.1371/journal.pntd.0003780>
- 943 Vega-Rúa A, Marconcini M, Madec Y, Manni M, Carraretto D, Gomulski LM, Gasperi G, Failloux A-B,
944 Malacrida AR (2020) Vector competence of *Aedes albopictus* populations for chikungunya virus is
945 shaped by their demographic history. *Communications Biology*, **3**, 326.
946 <https://doi.org/10.1038/s42003-020-1046-6>
- 947 Vega-Rúa A, Schmitt C, Bonne I, Locker JK, Failloux A-B (2015) Chikungunya Virus Replication in Salivary
948 Glands of the Mosquito *Aedes albopictus*. *Viruses*, **7**, 5902–5907. <https://doi.org/10.3390/v7112917>
- 949 Vega-Rúa A, Zouache K, Caro V, Diancourt L, Delaunay P, Grandadam M, Failloux A-B (2013) High
950 Efficiency of Temperate *Aedes albopictus* to Transmit Chikungunya and Dengue Viruses in the
951 Southeast of France. *PLoS ONE*, **8**, e59716. <https://doi.org/10.1371/journal.pone.0059716>
- 952 Venturi G, Luca MD, Fortuna C, Remoli ME, Riccardo F, Severini F, Toma L, Manso MD, Benedetti E,
953 Caporali MG, Amendola A, Fiorentini C, Liberato CD, Giammattei R, Romi R, Pezzotti P, Rezza G, Rizzo
954 C (2017) Detection of a chikungunya outbreak in Central Italy, August to September 2017.
955 *Eurosurveillance*, **22**, 17–00646. <https://doi.org/10.2807/1560-7917.es.2017.22.39.17-00646>
- 956 Viglietta M, Bellone R, Blisnick AA, Failloux A-B (2021) Vector Specificity of Arbovirus Transmission.
957 *Frontiers in Microbiology*, **12**, 773211. <https://doi.org/10.3389/fmicb.2021.773211>
- 958 Wagar ZL, Tree MO, Mpoy MC, Conway MJ (2017) Low density lipopolyprotein inhibits *flavivirus*
959 acquisition in *Aedes aegypti*. *Insect Molecular Biology*, **26**, 734–742.
960 <https://doi.org/10.1111/imb.12334>
- 961 Wickham H, Averick M, Bryan J, Chang W, McGowan L, François R, Golemund G, Hayes A, Henry L,
962 Hester J, Kuhn M, Pedersen T, Miller E, Bache S, Müller K, Ooms J, Robinson D, Seidel D, Spinu V,
963 Takahashi K, Vaughan D, Wilke C, Woo K, Yutani H (2019) Welcome to the Tidyverse. *Journal of Open*
964 *Source Software*, **4**, 1686. <https://doi.org/10.21105/joss.01686>
- 965 Williams AE, Franz AWE, Reid WR, Olson KE (2020) Antiviral Effectors and Gene Drive Strategies for
966 Mosquito Population Suppression or Replacement to Mitigate Arbovirus Transmission by *Aedes*
967 *aegypti*. *Insects*, **11**, 52. <https://doi.org/10.3390/insects11010052>
- 968 Wimberly MC, Davis JK, Evans MV, Hess A, Newberry PM, Solano-Asamoah N, Murdock CC (2020) Land
969 cover affects microclimate and temperature suitability for arbovirus transmission in an urban
970 landscape. *PLoS Neglected Tropical Diseases*, **14**, e0008614.
971 <https://doi.org/10.1371/journal.pntd.0008614>
- 972 Zhang Y, Yan H, Li X, Zhou D, Zhong M, Yang J, Zhao B, Fan X, Fan J, Shu J, Lu M, Jin X, Zhang E, Yan H
973 (2022) A high-dose inoculum size results in persistent viral infection and arthritis in mice infected with
974 chikungunya virus. *PLoS Neglected Tropical Diseases*, **16**, e0010149.
975 <https://doi.org/10.1371/journal.pntd.0010149>

- 976 Zhu Y, Zhang R, Zhang B, Zhao T, Wang P, Liang G, Cheng G (2017) Blood meal acquisition enhances
977 arbovirus replication in mosquitoes through activation of the GABAergic system. *Nature*
978 *Communications*, **8**, 1262. <https://doi.org/10.1038/s41467-017-01244-6>
- 979 Zouache K, Fontaine A, Vega-Rua A, Mousson L, Thiberge J-M, Lourenco-De-Oliveira R, Caro V,
980 Lambrechts L, Failloux A-B (2014) Three-way interactions between mosquito population, viral strain
981 and temperature underlying chikungunya virus transmission potential. *Proceedings of the Royal*
982 *Society B: Biological Sciences*, **281**, 20141078. <https://doi.org/10.1098/rspb.2014.1078>
- 983 Zouache K, Michelland RJ, Failloux A-B, Grundmann GL, Mavingui P (2012) Chikungunya virus impacts the
984 diversity of symbiotic bacteria in mosquito vector. *Molecular Ecology*, **21**, 2297–2309.
985 <https://doi.org/10.1111/j.1365-294x.2012.05526.x>
- 986